INFORMATION TO USERS

This manuscript has been reproduced from the microfilm master. UMI films the text directly from the original or copy submitted. Thus, some thesis and dissertation copies are in typewriter face, while others may be from any type of computer printer.

The quality of this reproduction is dependent upon the quality of the copy submitted. Broken or indistinct print, colored or poor quality illustrations and photographs, print bleedthrough, substandard margins, and improper alignment can adversely affect reproduction.

In the unlikely event that the author did not send UMI a complete manuscript and there are missing pages, these will be noted. Also, if unauthorized copyright material had to be removed, a note will indicate the deletion.

Oversize materials (e.g., maps, drawings, charts) are reproduced by sectioning the original, beginning at the upper left-hand corner and continuing from left to right in equal sections with small overlaps.

Photographs included in the original manuscript have been reproduced xerographically in this copy. Higher quality 6" x 9" black and white photographic prints are available for any photographs or illustrations appearing in this copy for an additional charge. Contact UMI directly to order.

Bell & Howell Information and Learning
300 North Zeeb Road, Ann Arbor, MI 48106-1346 USA
800-521-0600

Université d'Ottawa · University of Ottawa

Modeling Free-Radical Polymerizations with Depropagation using Java™: Methyl Methacrylate/α-methylstyrene at Elevated Temperatures

by

Christopher Badeen

A thesis
submitted to the Faculty of Graduate and Post-Doctoral Studies
in partial fulfillment of the requirements for the degree of

Master of Applied Science
in
Chemical Engineering

Department of Chemical Engineering
University of Ottawa

Abstract

There is growing interest in polymerization reactions at elevated temperatures due to potential advantages of elevated-temperature operation. However, most studies to date have focused on polymerization reactions at relatively low temperatures (i.e., below 80°C). This study of the copolymerization of methyl methacrylate (MMA) and α-methylstyrene (α-ms) at elevated temperatures (100 – 140°C), is in response to both the growing interest in the area of elevated temperature polymerization and the scarcity of knowledge in this area.

A computer program was written in the Java™ programming language to simulate the copolymerization being investigated. This is the first published use of Java™ to write a numerical polymerization simulation program. The program implements the model for free-radical polymerization described in Dubé et al. (1997), but with modifications to account for reverse polymerization reactions. The model described by Kruger (1987) was used to account for reversible polymerization reactions.

Results from the program are compared with full conversion data acquired during this study and other published data. It was found that the program was able to provide good results for conversion versus both time and copolymer composition for the MMA/α-ms copolymer system, but only in regions where diffusion-controlled termination effects were negligible. The match between simulation data generated by the program and experimental data was poor in regions where diffusion-controlled termination effects were significant due largely to the program's inability to make accurate molecular weight predictions for the MMA/α-ms copolymer system.

The results of this investigation indicate that the model used for this system shows promise. However, an alternative method for obtaining molecular weight predictions, particularly one that accounts for reversible reactions, should be sought. In addition, better parameter estimates for the Kruger model parameter R_A for MMA should be sought in order to improve the accuracy of the simulation predictions.

Abstrait

Il y a de l'intérêt dans le domaine des réactions de polymérisation aux températures élevées qui est en train de se développer à cause des avantages potentiels d'opérer à ces conditions. Cependant, la plupart des études jusqu'à maintenant se sont concentrées sur des réactions de polymérisation aux températures relativement basses (c'est à dire, au-dessous de 80°C). Cette étude de la copolymérisation du méthacrylate méthylique (MMA) et l'α-méthylstyrène (α-ms) aux températures élevées (100 - 140°C), est en réponse à l'intérêt croissant dans le domaine des polymérisations aux températures élevées et la pénurie de la connaissance dans ce domaine.

Un programme a été écrit dans le langage de programmation de Java™ pour simuler la copolymérisation étant étudiée. C'est la première fois publiée que Java™ a été utilisé pour écrire un programme capable de simuler des réactions de polymérisations. Le programme met en application le modèle pour la polymérisation libre-radicale décrite en Dubé *et al.* (1997), mais avec des modifications pour refléter les réactions réversibles de polymérisation. Le modèle décrit par Kruger (1987) a été employé pour modeler les réactions réversibles de polymérisation.

Les résultats du programme ont été comparés à un grand nombre de données de conversion mesurées durant cette étude et d'autres données provenant d'autres études. On a constaté que le programme pouvait fournir de bons résultats pour la conversion contre l'heure et la composition en copolymère pour la copolymérisation de MMA/α-ms, mais seulement dans les régions où les effets du control par diffusion étaient négligeables. Les résultats du programme dans les régions où les effets du control par diffusion étaient significatifs étaient pauvres à cause des calculs incorrects du poids moléculaire pour la copolymérisation du MMA/α-ms.

Les résultats de cette recherche indiquent que le modèle utilisé pour ce système se montre prometteur. Cependant, une méthode alternative pour obtenir les calculs du poids moléculaire, en particulier une qui explique bien les réactions réversibles, devrait être recherchée. En plus, de meilleures évaluations du paramètre R_A du modèle de Kruger pour MMA devraient être recherchées afin d'améliorer l'exactitude des prévisions générées par le programme.

Acknowledgments

I am indebted to a number of people for helping me during the preparation of this thesis. First and foremost I am indebted to my supervisor, Dr. Marc Dubé, who provided me with solid guidance throughout my time as a graduate student. Thanks Marc for your time and patience, and helping to make my studies immensely rewarding.

This project was the result of collaborative efforts with researchers at the University of Waterloo. Consultation with Dr. Alex Penlidis, Neil McManus, and Jun Gao provided invaluable help in choosing a direction for my research and validating the simulator. Thanks for taking the time to offer advice and answer the many question that were asked.

Thanks go out to those in the polymer group. Thanks to Tony for providing guidance how to do the polymerization experiments, and Hung for his help with the GPC work. To the entire group, thanks for your companionship and good humor throughout my stay.

Special thanks go to Louis Tremblay, without whom the experiments surely would have taken many additional months to complete.

Thanks go to my friends whose patience with my unpredictable work schedule was greatly appreciated.

Finally, thanks go to my parents, for the incredible support they've shown me during my studies.

Nomenclature

a	root-mean-square end-to-end distance per square root of the number of monomer units [dm]
A	adjustable free volume theory parameter [L]
C	parameter that modifies the rate of change of initiator efficiency [L]
C_{fcta}	constant for transfer to chain-transfer agent [dimensionless]
C_{fm}	constant for transfer to monomer [dimensionless]
C_{fmsi}	constant for transfer to monomer-soluble impurities [dimensionless]
C_{fp}	constant for transfer to polymer [dimensionless]
C_k	constant for internal double-bond reaction [dimensionless]
$[CTA]$	concentration of chain transfer agent [mol / L]
f	initiator efficiency factor [dimensionless]
f_0	initial initiator efficiency [dimensionless]
f_j	mole fraction of monomer j in reaction mixture [dimensionless]
j_c	entanglement spacing of pure polymer [number of monomer units]
F_j	instantaneous copolymer composition [mole fraction of monomer j]
$\overline{F}_j$	cumulative copolymer composition [mole fraction of monomer j]
k_d	initiator decomposition rate constant [min^{-1}]
k_{dp}	rate constant for depropagation [min^{-1}]
k_{dpo}	overall pseudo-kinetic rate constant for depropagation [min^{-1}]
k_{fcta}	overall rate constant for transfer to chain transfer agent [L mol^{-1} min^{-1}]
k_{fm}	overall rate constant for transfer to monomer [L mol^{-1} min^{-1}]
k_{fmsi}	overall rate constant for reaction with monomer soluble impurity [L mol^{-1} min^{-1}]
k_{fp}	overall rate constant for transfer to polymer [L mol^{-1} min^{-1}]
k_p	rate constant for propagation [L mol^{-1} min^{-1}]
k_{po}	overall pseudo-kinetic rate constant for propagation [L mol^{-1} min^{-1}]
$k_p^{\bullet}$	rate constant for reaction with terminal double bonds [L mol^{-1} min^{-1}]
$k_p^{\bullet\bullet}$	rate constant for reaction with internal double bonds [L mol^{-1} min^{-1}]
k_{dp}	rate constant for depropagation [min^{-1}]
k_t	overall termination rate constant [L mol^{-1} min^{-1}]
k_{to}	overall pseudo-kinetic termination rate constant [L mol^{-1} min^{-1}]
k_{tc}	rate constant for termination by combination [L mol^{-1} min^{-1}]
k_{tcrit}	critical termination rate constant [L mol^{-1} min^{-1}]
k_{td}	rate constant for termination by disproportionation [L mol^{-1} min^{-1}]
k_{trd}	reaction-diffusion control termination constant [L mol^{-1} min^{-1}]
k_{res}	"residual" reaction-diffusion control termination constant [L mol^{-1} min^{-1}]
k_z	rate constant for reaction with monomer soluble impurity [L mol^{-1} min^{-1}]
K	equilibrium constant for propagation [mol / L]
$K^{\bullet}$	constant for terminal double-bond reaction [dimensionless]

K_3	free volume theory parameter [g / mol]^m
i	represents monomer, polymer, and solvent [dimensionless]
$[I]$	concentration of initiator [mol / L]
m	adjustable free volume theory parameter [dimensionless]
$[M]$	concentration of monomer [mol / L]
$\overline{M}_n$	accumulated number-average molecular weight [g / mol]
$\overline{M}_w$	accumulated weight-average molecular weight [g / mol]
$\overline{M}_{wcrit}$	critical weight-average molecular weight [g / mol]
M_{weff}	effective molecular weight of monomer [g / mol]
$[MSI]$	concentration of monomer soluble impurity [mol / L]
n	adjustable free volume theory parameter [dimensionless]
N_A	Avogadro's number [molecules / mol]
N_{cta}	number of moles of chain transfer agent [mol]
N_m	number of moles of monomer [mol]
N_I	number of moles of initiator [mol]
Q_0, Q_1, Q_2	zeroeth, first, and second moments of the molecular weight distribution [mol / L]
R_I	overall rate of initiation [mol L^{-1} min^{-1}]
R_p	rate of polymerization [mol L^{-1} min^{-1}]
R_{po}	overall rate of polymerization [mol L^{-1} min^{-1}]
t	time [min]
T	temperature [K]
T_{gi}	glass transition temperature of species i [K]
V	volume of organic phase (monomer + polymer) [L]
V_i	volume of species i [L]
V_F	free volume [L]
V_{Fcrit}	critical free volume of initiator efficiency factor [L]
V_T	total volume of reaction mixture [L]
Y_0	concentration of free radicals [mol / L]
x	conversion [mass fraction]

Greek Letters

α_i	difference in the thermal expansion coefficients for species i above and below its glass transition temperature [K]
σ	Lennard-Jones diameter [dm]
γ	fraction of termination by disproportionation [dimensionless]

Table of Contents

Chapter 3 Experimental Methods and Product Characterization

Chapter 4 Modeling in Java

Chapter 5 Results and Discussion

Introduction

1.1 Introduction to Polymers and Polymerization Modeling

A polymer is a large molecule made up of smaller repeating units called monomers. For example, three units of the polymer polymethyl methacrylate are shown in Figure 1.1.1 below.

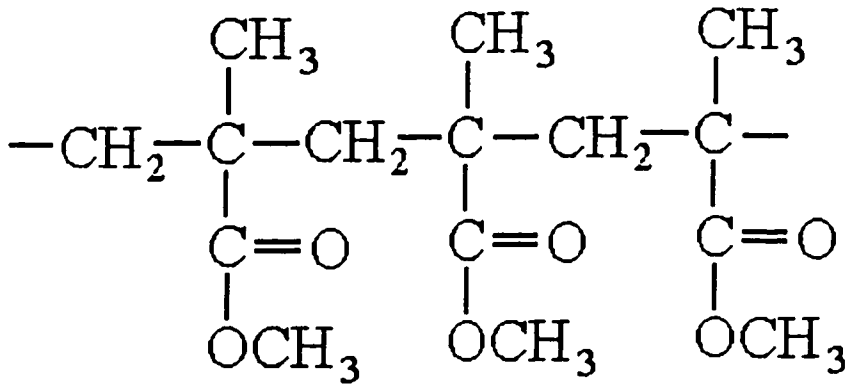

Figure 1.1.1 Three units of the polymer polymethyl methacrylate

Polymers are used in a wide variety of applications such as packaging, building and construction materials, automobile components, furnishings, and electrical components to name just a few. The versatility of polymers is in part due to the fact that many different polymers can be made, and their properties can be tailored to suit applications as required.

Some of the more important factors that affect the physical and chemical properties of polymers are: the type of monomer(s) used (functional groups,

functionality), polymer composition (functional groups, tacticity), and distribution of molecular weight. Polymers can be tailored to suit particular needs by the proper choice of monomer(s) and reaction conditions that will result in the desired polymer composition and molecular weight distribution.

Mathematical models of polymerization can be used to obtain predictions of both the composition and molecular weight of a polymer formed during the course of a polymerization reaction. The complexity of the most accurate models is such that analytical solutions are not feasible. However, the solution of the equations in complex models can be obtained in practice with the use of numerical methods implemented in computer code.

1.2 Uses of Polymerization Models

The ability of mathematical models of polymerization reactions to make predictions about the product of polymer reactions has many practical uses. A discussion of the usefulness of models is given by Gao and Penlidis (1996) and is summarized here.

1. Models enhance our process understanding since they can direct further research.
2. Models are useful for process design, parameter estimation, sensitivity analysis, and process simulation.
3. Models are useful for process optimization.
4. Models are useful for safety/venting considerations, and anticipation of worst-case scenarios.
5. Models are useful for optimal sensor selection and testing, sensor location, filtering and inference of unmeasured properties, and process control.
6. Since a model contains process knowledge that is transferable, interactive models (simulators) are useful for the education and training of personnel.

A polymerization model that provides predictions which adequately match real-world results can be employed for uses 2 - 6. In addition, a model that gives inadequate results is not without its uses. As implied in the first point, inadequate model predictions indicate a need for, and thus direct, further research.

1.3 Modeling Polymerizations at Elevated Temperatures

The majority of industrial scale polymerization reactions are carried out at relatively low temperatures (20° to 80°C). Not surprisingly, most of the published research has focused on studying polymerization reactions in this lower temperature range. However, there has recently been an increasing interest in studying polymerization reactions at elevated temperatures (80°C to 160°C). Carrying out polymerization reactions at elevated temperatures has significant benefits:

1) Productivity increases due to higher reaction rates.
2) The viscosity of the reaction medium is reduced at higher temperatures, resulting in greater ease of mixing and better heat transfer.
3) The initiator and chain transfer agent concentrations can be reduced, which results in cost savings and decreases residual impurities in the product.

In addition, knowledge of high temperature operation may be used to model hot-spots in a reactor for the case of lower temperature operation with imperfect mixing.

High temperature operation also has drawbacks:

1) Reactor operation may be more hazardous, requiring additional safety precautions.
2) Unwanted side reactions may be favored at higher temperatures.

3) The reverse polymerization reaction (depropagation) may become pronounced at higher temperatures thereby limiting theoretical maximum conversion significantly below 100%.

1.4 Thesis Objectives

The objectives of this thesis were threefold. The first was to implement a mechanistic model for free-radical polymerization in a computer program that could:

1) Simulate homopolymerization and copolymerization reactions in bulk and solution.
2) Simulate such reactions at both normal and elevated temperatures.
3) Simulate homopolymerization when the depropagation (reverse polymerization) reaction cannot be ignored.
4) Simulate copolymerization reactions when one or *both* monomers exhibit the effects of depropagation.

The second objective was to validate the simulation program with experimental data at normal and elevated temperatures for homopolymerization and copolymerization reactions in cases where depropagation reactions are not significant and in cases where depropagation effects cannot be ignored.

The third and final objective was to examine the suitability of the Java™ programming language for the development of the polymerization simulation program.

1.5 Thesis Outline

This thesis describes the development of a mathematical model of free-radical polymerization, implemented in the Java™ programming language, and its application to both the homopolymerization and copolymerization of the monomers α-methylstyrene and methyl methacrylate at normal and elevated temperatures.

Chapter 2 provides a description of free-radical polymerization reactions and the mathematical model used in the simulation program. A review of the literature relevant to this study is also provided.

Chapter 3 presents the experimental procedures and product characterization techniques employed to obtain experimental data on the methyl methacrylate/α-methylstyrene copolymer system.

Chapter 4 describes the Java™ programming language and why it was found to be a suitable language for developing the polymerization simulation program. The program and its validation are also discussed.

Chapter 5 presents the experimental results obtained during this investigation and compares the results with data generated by the simulation program. Additionally, experimental results from other sources are also compared with data generated by the program.

Chapter 6 summarizes the conclusions of the study and provides recommendations for future efforts in modeling the methyl methacrylate/α-methylstyrene copolymer system at elevated temperatures.

Model Development

The model described in this section consists of a set of differential and algebraic equations that describe the physical and chemical phenomena of free-radical polymerization. This discussion will be limited to bulk and solution polymerization in batch reactors, although the model can be extended to simulate emulsion polymerizations or polymerizations carried out in semibatch or continuous reactors. See Dubé *et al.* (1997) for extending the model to these cases.

2.1 Overview of Free-Radical Reactions

Free radical polymerizations are characterized by at least three reactions: initiation, propagation, and termination. Other reactions may occur, such as transfer reactions, branching reactions, and reactions with impurities.

The polymeric products of polymerization reactions alter the physical properties of the reaction medium, sometimes drastically. The changes in the reaction medium often have a significant impact on the kinetic parameters of a polymeric reaction, as well as the heat transfer parameters. Thus, when modeling polymer reactions, it is important to model both the chemical reactions occurring in the reaction medium as well as the impact of physical changes on kinetic parameters.

2.2 Initiation

Free-radical polymerization reactions begin with the creation of highly reactive free-radicals. This is accomplished by the decomposition of initiator

molecules by thermal or photochemical (ultra-violet) means. In bulk polymerization, the initiators are organic (monomer) soluble species such as 2,2'-azobis(isobutyronitrile) (AIBN). The decomposition reaction can be written as follows:

$$I_2 \xrightarrow{k_d} 2\,R_{IN}^{\bullet} \qquad (2.2.1)$$

where I_2 represents an initiator molecule, $R_{IN}^{\bullet}$ represents an initiator fragment (a free radical), and k_d represents the rate constant for the initiator decomposition reaction.

The fragments go on to react with monomer to produce primary radicals

$$R_{IN}^{\bullet} + M \xrightarrow{k_p'} R_1^{\bullet} \qquad (2.2.2)$$

M represents a monomer, $R_1^{\bullet}$ represents a primary radical, and k_p' represents the propagation rate constant for the addition of monomer to an initiator fragment.

The rate of initiation, R_I, is given by the expression

$$R_I = 2fk_d[I] \qquad (2.2.3)$$

where f is the initiator efficiency ($0 \leq f \leq 1$) and $[I]$ is the concentration of initiator. The need for the initiator efficiency term, f, is due to the fact that radicals produced in the decomposition reaction (2.2.1) may also undergo reactions to form neutral molecules instead of initiating polymerization. The initiator efficiency accounts for wastage of initiator due to such reactions. A more thorough explanation of the need of the initiator efficiency term can be found in texts on polymerization such as that by Odian (1991).

The initiator efficiency may not be constant throughout the full conversion range due to diffusion-control effects. That is, due to the increasing viscosity of the reaction mixture during polymerization, the mobility of species in the reaction

mixture may be reduced. The following semiemprical equation has been used to describe the changing initiator efficiency when the free volume of the reaction mixture (V_F) becomes less than a critical free volume, V_{fcrif}:

$$f = f_0 \exp(-C(1/V_F - 1/V_{Fcrif})) \tag{2.2.4}$$

where f_0 is the initial initiator efficiency and C is a parameter which modifies the rate of change of the efficiency. The critical free volume, V_{fcrif}, is dependent on temperature and initiator type.

2.3 Propagation

The reaction in which the length of a polymer chain increases by the addition of monomer is known as the propagation reaction. The reaction can be written as follows:

$$R_r^\bullet + M \xrightarrow{k_p} R_{r+1}^\bullet \tag{2.3.1}$$

where $R_r^\bullet$ is a radical of chain length r, and k_p is the rate constant for propagation. In the model, it is assumed that the propagation rate constant is independent of the polymer chain length.

The propagation rate constant, k_p, may not be constant throughout the full conversion range due to diffusion-control effects. In order to account for these effects, the model employs the following relation for k_p:

$$k_p = k_{p0} \exp\left(-B\left(\frac{1}{V_F} - \frac{1}{V_{Fpcrit}}\right)\right) \tag{2.3.2}$$

where k_{p0} is the propagation rate constant before diffusion-control effects occur, B is an adjustable parameter that depends on the monomer molecule type and V_{Fpcrit} is the critical free volume where the propagation reaction of the monomer becomes diffusion-controlled.

2.4 Termination

Radicals will mutually terminate to produce non-propagating species via termination reactions:

$$R_r^\bullet + R_s^\bullet \xrightarrow{k_{tc}} P_{r+s} \tag{2.4.1}$$

$$R_r^\bullet + R_s^\bullet \xrightarrow{k_{td}} P_r + P_s \tag{2.4.2}$$

where P_r is a polymer chain of length r, and k_{tc} and k_{td} are the rate constants for termination by combination and disproportionation, respectively. When termination occurs via the combination reaction illustrated by equation (2.4.1), a single larger polymer molecule is produced from the two polymer radicals. In contrast, when termination occurs via the disproportionation reaction illustrated by equation (2.4.2), two polymer molecules are produced, one saturated and one unsaturated. The presence of unsaturated polymer molecules allows the possibility of terminal double bond reactions. Terminal double bond reactions result in branching, an occurrence that may affect the molecular weight and physical properties of the polymer product.

The two rate constants for termination are related by the overall termination rate constant, k_t, and γ, the ratio of termination by disproportionation to the overall termination rate constant:

$$k_t = k_{tc} + k_{td} \tag{2.4.3}$$

$$\gamma = \frac{k_{td}}{k_t} \tag{2.4.4}$$

2.5 Chain Transfer Reactions

Termination by combination and disproportionation are not the only reactions that result in termination of growing polymer chains. A polymer radical may be terminated by the transfer of a hydrogen or other atom or species to it from another species in the reaction system. The species involved in such transfer reactions may be monomer, initiator, solvent, polymer, and/or chain transfer agent. Since chain transfer reactions result in premature termination of growing polymer chains (as compared to a case where such reactions are not present), the effect of chain transfer reactions is a reduction in polymer molecular weight. The effects of chain transfer to monomer, polymer, and chain transfer agents were included in the model, and will be described next.

Chain transfer to monomer is given by:

$$R_r^{\bullet} + M \xrightarrow{k_{fm}} P_r + M^{\bullet} \qquad (2.5.1)$$

where k_{fm} is the rate constant for transfer to monomer. This reaction results in terminal double bonds.

Chain transfer to polymer is given by:

$$R_r^{\bullet} + P_s \xrightarrow{k_{fp}} P_r + R_s^{\bullet} \qquad (2.5.2)$$

In this case, the radical chain of length r abstracts a hydrogen from the dead polymer chain of length s. It should be noted that chain transfer to polymer does not necessarily occur at the end of a dead polymer molecule.

Chain transfer to chain transfer agent, such as a mercaptan, is given by:

$$R_r^{\bullet} + RSH \xrightarrow{k_{fsa}} HP_r + RS^{\bullet} \qquad (2.5.3)$$

where RSH represents the chain-transfer agent which loses a labile hydrogen to the polymer radical. This reaction does not result in the formation of terminal double bonds. The $RS^{\bullet}$ radical will continue to propagate with monomer. Chain transfer agents are added to the reaction system in order to reduce molecular weights to desired levels.

2.6 Reactions with Double-Bonds

Radicals may undergo reactions with internal and terminal double-bonds when these types of atomic bonds are present. The rate constant for terminal double-bond reactions is $k_p^{\bullet}$ and that for internal double-bond reactions is $k_p^{\bullet\bullet}$.

$$R_{n,i}^{\bullet} + P_m \xrightarrow{k_p^{\bullet}} R_{m+n,i}^{\bullet} \tag{2.6.1}$$

$$R_{n,i}^{\bullet} + P_m \xrightarrow{k_p^{\bullet\bullet}} R_{m+n,i}^{\bullet} \tag{2.6.2}$$

Terminal double-bond reactions yield trifunctional branch points, whereas internal double-bond reactions yield tetrafunctional branch points.

2.7 Reaction with Impurities

Radicals may react with monomer-soluble impurities (MSI), terminating the growth of polymer chains. These impurities include free-radical inhibitors such as hydroquinone and *tert*-butylcatechol (TBC). Monomer manufacturers typically add inhibitors to freshly produced monomers in order to prevent uncontrolled and potentially dangerous polymerization of the monomers while in storage.

$$R^{\bullet}_{n,i} + MSI \xrightarrow{k_{fmsi}} P(MSI) \qquad (2.7.1)$$

In the equation above, k_{fmsi} is the rate constant for the reaction of monomer-soluble impurity with radicals ending in monomer *i*. As was suggested by Dubé *et al.* (1997), the rate constant k_{fmsi} was assumed to be identical for all monomers in order to simplify the model.

2.8 Depropagation

Polymerization reactions can often be treated as proceeding in one direction only, so that the equation for propagation is sufficient to describe the growth of polymer chains:

$$R^{\bullet}_{r} + M \xrightarrow{k_p} R^{\bullet}_{r+1} \qquad (2.8.1)$$

Under certain conditions, the reverse reaction, depropagation, may also be important:

$$R^{\bullet}_{r} + M \xleftarrow[k_{dp}]{} R^{\bullet}_{r+1} \qquad (2.8.2)$$

If the entropy and enthalpy of polymerization are both negative, polymerization will begin only when the temperature of the system is lowered below a "ceiling temperature". At the ceiling temperature, the rate of propagation equals the rate of depropagation. At or above the ceiling temperature, no high molecular weight polymer can be formed. If the system is sufficiently far below the ceiling temperature, the effects of depropagation may be ignored with very little loss of accuracy.

The rate constants for propagation and depropagation are related by the equilibrium constant, K:

$$K = \frac{k_{dp}}{k_p} \tag{2.8.3}$$

The value of K is identical to the concentration of monomer in the system at equilibrium.

2.9 Rate Equations and Material Balances

Material balances on a reaction system yield expressions for the rate of disappearance or accumulation of the various species in the reaction system.

The rate of polymerization, R_p, is given by:

$$R_p = [M]k_p \sum_{r=1}^{\infty} R_r^{\bullet} - k_{dp} \sum_{r=2}^{\infty} R_r^{\bullet} \tag{2.9.1}$$

However, it would be computationally prohibitive to implement the equation above in a program because it would require the program to keep track of the chain length of all of the radicals in the system. The following approximate equation was used instead:

$$R_p = [M]k_p \sum_{r=1}^{\infty} R_r^{\bullet} - k_{dp} \sum_{r=1}^{\infty} R_r^{\bullet} \tag{2.9.2}$$

Note that in the first case, the second summation is from 2 to ∞, while in the second case the summation is from 1 to ∞. The approximation being made is that the concentration of primary radicals is negligible in comparison to the overall concentration of free-radicals in the system. This approximation will generally be valid unless the reaction is being carried out very near the ceiling temperature. The approximate equation can also be rewritten as:

$$R_p = [M]k_p Y_o - k_{dp} Y_o \tag{2.9.3}$$

where Y_o is the concentration of free radicals in the system.

The concentration of free radicals in the system is given by:

$$Y_o = \frac{\left(\sum_{i=1}^{N_z} k_{zi}^2 [MSI]_i^2 + 4k_t R_I\right)^{\frac{1}{2}} - \sum_{i=1}^{N_z} k_{zi} [MSI]_i}{k_t} \tag{2.9.4}$$

where N_z is the number of monomer soluble impurities in the system, k_z is the rate constant for reaction with monomer soluble impurity, and $[MSI]$ is the concentration of monomer-soluble impurity.

Material balances on a batch reactor yield the following expressions.

A balance on the initiator gives:

$$\frac{dN_I}{dt} = -k_d N_I \tag{2.9.5}$$

where N_I is the number of moles of initiator present in the system at time t. A balance on the monomer yields:

$$\frac{dN_m}{dt} = -R_p V \tag{2.9.6}$$

where N_m is the number of moles of monomer, and V is the volume of the organic phase (monomer + polymer + solvent when applicable). A balance on the chain transfer agent yields:

$$\frac{dN_{cta}}{dt} = -k_{fcta}[CTA]Y_0V \tag{2.9.7}$$

where N_{cta} is the number of moles of chain transfer agent, and $[CTA]$ is the concentration of chain transfer agent. A balance on the monomer-soluble impurities yields:

$$\frac{dN_{msi}}{dt} = -k_{fmsi}[MSI]Y_0V \tag{2.9.8}$$

where N_{msi} is the number of moles of monomer soluble impurity, and $[MSI]$ is the concentration of monomer-soluble impurity.

2.10 Multicomponent Polymerizations

The discussion thus far has been limited to homopolymerization reactions, i.e. reactions in which a polymer is produced from a single monomer. However, many industrially important polymer products are produced from two or more monomers. By producing polymers from a mixture of monomers, one may combine desirable characteristics of two or more polymers into a single polymer product. The propagation equations for copolymerization are as follows:

$$\begin{aligned}
R^{\bullet}_{r,1} + M_1 &\underset{k_{dp11}}{\overset{k_{p11}}{\rightleftharpoons}} R^{\bullet}_{r+1,11} \\
R^{\bullet}_{r,1} + M_2 &\underset{k_{dp12}}{\overset{k_{p12}}{\rightleftharpoons}} R^{\bullet}_{r+1,12} \\
R^{\bullet}_{r,2} + M_1 &\underset{k_{dp21}}{\overset{k_{p21}}{\rightleftharpoons}} R^{\bullet}_{r+1,21} \\
R^{\bullet}_{r,2} + M_2 &\underset{k_{dp22}}{\overset{k_{p22}}{\rightleftharpoons}} R^{\bullet}_{r+1,22}
\end{aligned} \tag{2.10.1}$$

The equations above implicitly state that the terminal model for polymerization is being used. In other words, the forward rate of reaction of a growing polymer chain is assumed to depend only on the type of monomer on the chain that bears a free-radical.

When modeling multicomponent polymerization reactions, it is useful to define overall rate constants. The overall propagation pseudo-kinetic rate constant for an N-component polymerization can be defined as (Hamielec *et al.*, 1987; Dubé *et al.*, 1997):

$$k_{po} = \sum_{i=1}^{N}\sum_{j=1}^{N} k_{pij}\phi_i f_j \tag{2.10.2}$$

For a copolymerization reaction, the ϕ values are as follows:

$$\phi_1 = \frac{k_{p21} f_1}{\psi} \tag{2.10.3}$$

$$\phi_2 = 1 - \phi_1 = \frac{k_{p12} f_2}{\psi} \tag{2.10.4}$$

$$\psi = k_{p21} f_1 + k_{p12} f_2 \tag{2.10.5}$$

The overall termination pseudo-kinetic rate constant may be defined as:

$$k_{to} = \sum_{i=1}^{N}\sum_{j=1}^{N} k_{toij}\phi_i\phi_j \tag{2.10.6}$$

As suggested by Dubé *et al.* (1997), the cross-termination rate constant was defined as:

$$k_{toij} = k_{toi} F_i + k_{toj} F_j \tag{2.10.7}$$

where F_i is the instantaneous copolymer composition. The overall γ value was calculated as:

$$\gamma_o = \gamma_1 F_1 + \gamma_2 F_2 \tag{2.10.8}$$

An overall chain transfer to CTA pseudo-kinetic rate constant was calculated as:

$$k_{fcta} = \sum_{j=1}^{N} k_{fctaj} \phi_j \tag{2.10.9}$$

An overall pseudo-kinetic rate constant for transfer to monomer was calculated as:

$$k_{fm} = \sum_{i=1}^{N} \sum_{j=1}^{N} k_{fmij} \phi_i f_j \tag{2.10.10}$$

An overall pseudo-kinetic rate constant for transfer to polymer was calculated as:

$$k_{fp} = \sum_{i=1}^{N} \sum_{j=1}^{N} k_{fpij} \overline{F}_j \phi_i \tag{2.10.11}$$

An overall pseudo-kinetic rate constant for terminal double bond reactions, $k_p^{\bullet}$, was calculated as:

$$k_p^{\bullet} = \sum_{i=1}^{N} \sum_{j=1}^{N} k_{pij}^{\bullet} \overline{F}_j \phi_i \tag{2.10.12}$$

Similarly, an overall pseudo-kinetic rate constant for internal double bond reactions, $k_p^{\bullet\bullet}$, was calculated as:

$$k_p^{\bullet\bullet} = \sum_{i=1}^{N}\sum_{j=1}^{N} k_{pij}^{\bullet\bullet} \overline{F}_j \phi_i \qquad (2.10.13)$$

When depropagation effects are ignored, polymerization rates for individual monomer species are defined as:

$$R_{pj} = Y_o[M] f_j \sum_{j=1}^{N} k_{pij} \phi_i \qquad (2.10.14)$$

The overall rate of polymerization, R_{po}, can be obtained as the sum of the rates of polymerization of the individual species, or as

$$R_{po} = Y_o[M] k_{po} \qquad (2.10.15)$$

For cases when depropagation effects are not ignored, the individual polymerization rates are obtained by the method described by Kruger (1987). The derivation and equations for Kruger's model for copolymerization reactions with depropagation are presented in Appendix A.

The overall depropagation rate constant was defined as

$$k_{dpo} = \frac{\begin{array}{c}\text{Overall rate of polymerization if no depropagation were to occur} \\ - \text{Overall rate of polymerization with depropagation}\end{array}}{Y_o} \qquad (2.10.16)$$

The instantaneous copolymer composition is calculated as:

$$F_j = \frac{R_{pj}}{\sum_{j=1}^{N} R_{pj}} \qquad (2.10.17)$$

The cumulative copolymer composition is calculated as:

$$\overline{F}_j = \frac{N_{\text{pol}j}}{\sum_{j=1}^{N} N_{\text{pol}j}} \tag{2.10.18}$$

2.11 Molecular Weight Calculations

As mentioned in the introduction, polymerization reactions result in a polymer product having a distribution of molecular weights. The distribution can be characterized by molecular weight averages such as the number-average molecular weight, $\overline{M}_n$, and the weight-average molecular weight, $\overline{M}_w$. These quantities are defined as follows:

$$\overline{M}_n = \frac{w}{\sum N_x} = \frac{\sum N_x M_x}{\sum N_x} \tag{2.11.1}$$

where the summations are over all the different chain lengths of polymer molecules from $x = 1$ to $x = \infty$, w is the total weight of polymers in a polymer sample, and N_x is the number polymer molecules in the sample with molecular weight M_x.

$$\overline{M}_w = \sum w_x M_x = \frac{\sum N_x M_x^2}{\sum N_x M_x} \tag{2.11.2}$$

where w_x is the weight fraction of polymer molecules whose molecular weight is M_x. It should be noted that equations above for the molecular weight averages apply only to linear polymers and not to branched polymers.

When the full molecular weight distribution is not required and molecular weight averages are sufficient, the method of moments can be used. By invoking the stationary-state hypothesis for radicals, one can derive the following moment equations (Ray, 1972; Broadhead *et al.*, 1985; Hamielec *et al.*, 1987; Xie and Hamielec, 1993a,b) and obtain the leading moments of the distribution (Q_0, Q_1, Q_2):

$$\frac{dVQ_0}{dt} = \left(\tau + \beta/2 - \frac{C_k Q_1}{[M]} - \frac{K^* Q_1}{[M]} \right) k_p [M] Y_o V \tag{2.11.3}$$

$$\frac{dVQ_1}{dt} = \left(1 + C_{fm} + \frac{C_{fcta}[CTA]}{[M]} + \frac{C_{fmsi}[MSI]}{[M]} \right) k_p [M] Y_o V \tag{2.11.4}$$

$$\frac{dVQ_2}{dt} = \left(\text{factor} + 2\left(1 + \frac{K^* Q_1 + C_k Q_2}{[M]} \right) \frac{\text{bracket}}{\text{denom}} + \beta \left(\frac{\text{bracket}}{\text{denom}} \right)^2 \right) k_p [M] Y_o V \tag{2.11.5}$$

where

$$\tau = \frac{k_{td} Y_0}{k_p [M]} + C_{fm} + \frac{C_{fcta}[CTA]}{[M]} + \frac{C_{fmsi}[MSI]}{[M]} \tag{2.11.6}$$

$$\beta = \frac{k_{tc} Y_o}{k_p [M]} \tag{2.11.7}$$

$$\text{factor} = 1 + C_{fm} + \frac{C_{fcta}[CTA]}{[M]} + \frac{C_{fmsi}[MSI]}{[M]} \tag{2.11.8}$$

$$\text{denom} = \tau + \beta + \frac{C_{fp} Q_1}{[M]} \tag{2.11.9}$$

$$\text{bracket} = 1 + C_{fm} + \frac{(C_{fp} + C_k) Q_2}{[M]} + \frac{K^* Q_1}{[M[} + \frac{C_{fcta}[CTA]}{[M]} + \frac{C_{fmsi}[MSI]}{[M]} \tag{2.11.10}$$

C_{fm}, C_{fcta}, and C_{fmsi} are the constants for transfer to monomer, to chain-transfer agent, and to monomer-soluble impurities, respectively. They are defined as:

$$C_{fin} = k_{fin} / k_p \tag{2.11.11}$$

$$C_{feta} = k_{feta} / k_p \tag{2.11.12}$$

$$C_{finst} = k_{finst} / k_p \tag{2.11.13}$$

C_{fp}, C_k, and $K^{\bullet}$ are the constants for transfer to polymer, internal double-bond, and terminal double-bond reactions, respectively. They are defined as:

$$C_{fp} = k_{fp} / k_p \tag{2.11.14}$$

$$C_k = k_p^{\bullet\bullet} / k_p \tag{2.11.15}$$

$$K^{\bullet} = k_p^{\bullet} / k_p \tag{2.11.16}$$

The accumulated number- and weight-average molecular weights are calculated by evaluating

$$\overline{M}_n = \frac{Q_1}{Q_0} M_{weff} \tag{2.11.17}$$

$$\overline{M}_w = \frac{Q_2}{Q_1} M_{weff} \tag{2.11.18}$$

where M_{weff} is the effective monomer molecular weight. For a homopolymer system, M_{weff} is the molecular weight of the monomer. For multicomponent systems, M_{weff} is calculated by summing the individual monomer molecular weights and weighting them by the cumulative polymer composition. Also, overall rate constants are used when the equations are applied to multicomponent systems.

The molecular weight moment equations above are derived under the assumption of irreversible propagation reactions. A correction was applied to the molecular weight equations in an attempt to account for depropagation reactions. Each occurrence of the term $k_p[M]$ was replaced with the term $k_p[M] - k_{dp}$.

2.12 Diffusion-Controlled Termination

Many polymerizations are characterized by an autoacceleration period – a period during which the reaction rate increases (often dramatically) with conversion, even under isothermal conditions. The occurrence of this period can be explained as follows. The viscosity of the reaction medium increases as the polymer concentration (conversion) increases, due to the relatively high viscosity of most polymers as compared to the monomers from which they are produced. This, in turn, will result in a decrease in the rate of translational diffusion of polymer radicals (i.e., the rate of movement of whole radicals towards one another decreases). Due to the decreased rate of translational diffusion of radicals, the rate of polymer radical termination decreases and the rate of polymerization increases as a result. Since the rate of polymerization increases, the rate at which the viscosity of the medium increases as well, accelerating the rate of polymerization further. This effect is commonly referred to as the gel or auto-acceleration effect. The terms Trommmsdorf effect or Norrish-Smith effect are also used in recognition of the early workers' contributions to this subject.

The free volume approach of Marten and Hamielec (1979) was used to take the gel effect into account. For the sake of brevity, the explanation of most symbols will be omitted from the text but can be found in the nomenclature list.

$$K_3 = \overline{M}_{wcrit}^{m} e^{\left(A/V_{Fcrit}\right)} \tag{2.12.1}$$

$$V_F = \sum_{i=1}^{N} \left(0.025 + \alpha_i \left(T - T_{gi}\right)\right) \frac{V_i}{V_T} \tag{2.12.2}$$

$$k_T = k_{tcrit} \left(\frac{\overline{M}_{wcrit}}{\overline{M}_w} \right)^n e^{\left(-A\left(\frac{1}{V_F} - \frac{1}{V_{Fcrit}}\right)\right)} \tag{2.12.3}$$

In the program, the termination rate constant k_t remains constant until the value of K_3 from equation (2.12.1) is found to equal (or exceed) a temperature

dependent "flag" value for K_3 that signals the onset of the gel effect. When the "flag" value is reached, the following values are fixed:

$$\overline{M}_{wcrit} = \overline{M}_w \tag{2.12.4}$$

$$V_{Fcrit} = V_F \tag{2.12.5}$$

$$k_{tcrit} = k_t \tag{2.12.6}$$

The termination rate constant is then calculated as the sum of the termination rate constants from equation (2.12.3) above, and equation (2.12.9) below. When the reaction medium becomes extremely viscous, the reaction-diffusion control constant, k_{trd}, becomes important. The method of Russell *et al.* (1988) was used to calculate k_{trd}. The method employs the following equations:

$$k_{tres,min} = \frac{4}{3}\pi N_A k_p [M] a^2 \sigma \tag{2.12.7}$$

$$k_{tres,max} = \frac{8}{3}\pi N_A k_p [M] a^2 j_c^{1/2} \tag{2.12.8}$$

$$k_{trd} = k_{tres,min} x + k_{tres,max}(1-x) \tag{2.12.9}$$

For multicomponent systems, overall rate constants are used. In addition, weighted averages (weighted by instantaneous polymer composition) of free volume parameters were used for multicomponent systems.

2.13 Assumptions

In the development of the model, many assumptions were implicitly made. The following is a list of significant assumptions:

1. All rate constants are independent of chain length.
2. The stationary-state hypothesis for radicals is valid. That is, the rate of change in free radical concentration with respect to time is very small.

For the implementation of the model in the simulation program, further assumptions were made. The following is a list of these assumptions:

1. There is perfect mixing in the reactor. That is, the reactor is completely homogeneous.
2. The reaction is carried out isothermally.
3. The densities of polymer and monomer are additive.

2.14 Literature Review

2.14.1 Homopolymerization and Copolymerization at Elevated Temperatures

Studies of the homopolymerization behavior of individual monomers can yield many of the model parameters that are essential to modeling copolymerization behavior. A substantial amount of literature is devoted to the study of the polymerization of methyl methacrylate in both homopolymer and copolymer forms. However, the vast majority of this work has been at temperatures at or below 80°C. The review article by Gao and Penlidis (1996) presented a comprehensive report on the homopolymerization of methyl methacrylate at or below 90°C. In a more recent article, Gao and Penlidis (1998) presented a comprehensive report on the

copolymerization behavior of methyl methacrylate in several copolymer systems for temperatures at or below 80°C.

Hoppe and Renken (1998) presented a mechanistic model that gives a good kinetic representation of the homopolymerization of MMA in the temperature range of 20-165°C. Experimental data from several sources were compared with simulation predictions obtained using their model.

Weickert (1998) discussed the high temperature polymerization of MMA as it relates to the hollow shaft reactor that he designed. He noted that 100% conversion cannot be achieved because conversion is limited by glass transition issues below roughly 110°C and equilibrium limitations above 110°C.

Direct measurements of homopolymerization data for the *free-radical* polymerization of α-methylstyrene (α-ms) are not available in the literature. The reason for the complete lack of data is that the homopolymerization rate of α-ms below its ceiling temperature of 61°C is extremely low, and it is impossible to produce homopolymer at or above the ceiling temperature without applying substantial amounts of pressure. It is possible to produce α-ms homopolymer by *anionic* polymerization, as has been reported in articles such as Zhuang *et al.* (1997). However, the kinetics of anionic polymerization are too different from free-radical polymerization to be useful to this study.

In the absence of directly measured homopolymerization data, free-radical homopolymerization data for α-ms may be extracted from copolymerization data. Kukulj and Davis (1998) estimated the propagation rate constant, k_p, for α-ms homopolymerization from styrene/α-ms copolymerization data that they measured by pulsed-laser techniques. The pulsed-laser polymerization technique is currently recognized as the most reliable means of measuring the propagation rate constant.

2.14.2 Copolymerization of Methyl Methacrylate and α-methylstyrene

A considerable amount of research has been made for the copolymerization of MMA and α-ms. However, the majority of this research was conducted at temperatures below the lowest temperature of interest in this investigation (100°C).

The reason that high temperature work has been neglected is that below 100°C, α-ms clearly exhibits depropagation effects while MMA does not. As a result, simplified models for copolymerization with depropagation can be used which need to take into account the depropagation of α-ms only.

Early work in the kinetic analysis of reversible copolymerization was conducted by Lowry (1960). Lowry described three models of the effects of depropagation on copolymer composition. Other workers (O'Driscoll and Gasparro, 1967) and (Ivin and Spensley, 1967) later confirmed the applicability of Lowry's second model (case II) for a variety of systems where only one of the monomers depropagates.

Wittmer (1971) introduced his own model for reversible copolymerization and tried to determine parameters for his model using experimental data for the MMA/α-ms copolymer system. Copolymerization data for the MMA/α-ms from 20 to 150°C was provided.

The topic of copolymerization with depropagation is examined in a series of ten articles co-authored by O'Driscoll. In the fifth (Izu and O'Driscoll, 1970) and seventh article (Izu *et al.*, 1972) in the series, comparisons are made between model predictions of copolymer composition to experimental data for the MMA/α-ms copolymer system. The probabilistic approach used to predict copolymer composition, which was valid in cases where one or both monomers exhibit depropagation, was described in the third article in the series (Howell *et al.*, 1970). A method for predicting molecular weight-averages based on using generating functions is described in the ninth article in the series (Kang and O'Driscoll, 1973).

Ito and Kodaira (1986) calculated reactivity ratios and equilibrium constants for the MMA/α-ms copolymer system. These parameters were estimated from their own data and that of Wittmer (1971).

Martinet and Guillot published a series of three articles on the copolymerization of MMA/α-ms. In the first article (Martinet and Guillot, 1997), a model was developed and compared to solution copolymerization data at 60°C. In the second article (Martinet and Guillot, 1999a) the model developed in the first article was compared to bulk polymerization data for MMA/α-ms obtained at 50, 60

and 80°C. The third article in the series (Martinet and Guillot, 1999b) explored the emulsion polymerization kinetics of the MMA/α-ms system at 60, 70, and 85°C.

Palmer (1999) examined the use of Wittmer's model and the one developed by Kruger *et al.* (1987) to describe the composition of MMA /α-ms copolymers produced at elevated temperatures (up to 140°C). Palmer used experimental data to determine reactivity ratios as well as parameters for the Wittmer and Kruger models. He found that both models yielded identical results when both of their model equations converged. However, Kruger's model was found to be numerically stable over a broad range of feed compositions while Wittmer's model would not converge at high α-ms feed levels. Predictions of copolymer composition made using Kruger's model were compared with experimental MMA/α-ms copolymerization data for both bulk and solution polymerizations at 115 and 140°C. Kruger's model was found to give excellent predictions of copolymer composition for the MMA/α-ms copolymer system.

Examination of the articles in the literature reveals that there are no published articles describing attempts to simulate the conversion profile of a polymerization reaction where the depropagation of one or *both* monomers cannot be ignored. In order to address this issue, an attempt was made to simulate the conversion, molecular weight, and copolymer composition of MMA /α-ms copolymers in cases where the depropagation of one or both monomers could not be ignored. Thus, this thesis is the first published attempt to simulate the conversion profile of a polymerization reaction where the depropagation of one or *both* monomers cannot be ignored.

Experimental Methods and Product Characterization

This chapter describes the full conversion copolymerization experiments that were carried out with the monomers α-methylstyrene (α-MS) and methyl methacrylate (MMA). The experimental procedure was based on the standard methods described by Stickler (1987). Data collected include conversion versus time, polymer composition, and molecular weight. This chapter begins with a description of the monomer purification procedure, and is followed by a description of the procedure used to polymerize the monomers and isolate polymer samples. The characterization methods for obtaining polymer composition and molecular weight distributions are also described.

3.1 List of Reagents

The following is a list of the reagents used to carry out the study.

Monomers:

α-methylstyrene (α-ms, Aldrich Chemical Co., inhibited with 15 ppm p-TBC)
Methyl methacrylate (MMA, Aldrich Chemical Co., inhibited with 10-100 ppm MEHQ)

Initiator:

Di-tert-butyl peroxide (Trigonox-B, Akzo Nobel Chemicals Inc.)

Solvents:

Acetone (Reagent Grade, ACP Chemicals Inc.)
Chloroform-D (Cambridge Isotope Laboratories)
Hexanes (Reagent Grade, ACP Chemicals Inc.)
Tetrahydrofuran (THF, HPLC grade, VWR Canlab Inc.)

Other:

Sodium hydroxide pellets (lab grade, ACP Chemicals Inc.)
Calcium chloride Anhydrous (4-20 mesh, lab grade, ACP Chemicals Inc.)
Hydroquinone (Baker grade, J.T. Baker Chemical Co.)

3.2 Monomer Purification

The monomers were purified before use. Monomer purification was carried out in three steps. The first step was the removal of free-radical inhibitors by washing with a sodium hydroxide solution. Monomer manufacturers typically add inhibitors to freshly produced monomers in order to prevent uncontrolled and potentially dangerous polymerization of the monomers while in storage. The second step was the distillation of the monomer. The third and final step was the removal of oxygen (a free radical inhibitor) by a vacuum apparatus.

3.2.1 Removal of Inhibitor

Each of the monomers was washed three times with a 10 wt% sodium hydroxide solution to remove the radical inhibitors. A volume of sodium hydroxide solution equal to about one tenth the volume of monomer was used for each wash. In a similar fashion, the monomers were then rinsed three times with double-distilled de-ionized water to remove trace sodium hydroxide. The monomers were then dried by

the addition of anhydrous calcium chloride pellets. The monomers were stored in a freezer (-10°C) before undergoing the distillation procedure described below.

3.2.2 Distillation

Immediately before use, each monomer was distilled under vacuum to remove trace impurities. Distillation was carried out using a rotary evaporator. Each monomer was removed from the freezer and allowed to reach room temperature before being placed in the rotary evaporator. This prevented moisture in the air from condensing inside the monomer containers. For MMA, roughly 100mL of monomer was placed in the evaporating flask. The evaporating flask, rotating at 150-200 rpm, was submerged into a water bath at 25°C. Vacuum was then applied to the apparatus. The first 20-30mL of condensate to form in the receiving flask were discarded, and the distillation was allowed to proceed until only 20-30mL of monomer remained in the evaporating flask. The distilled monomer in the receiving flask was then stored in a freezer for a maximum of 24 hours before the polymerization experiments in order to minimize the formation of dimers and trimers. The distillation procedure for α-ms was similar to that of MMA except the quantities of monomer were halved, and the water bath was at a temperature of 85°C.

3.2.3 Solution Preparation and Oxygen Removal

All solutions were prepared on a mass basis. Polymerization reactions were carried out in borosilicate glass ampoules (length 10 cm, outer diameter 1.7cm, capacity 10 mL). Approximately 3mL of solution was placed in each ampoule. The ampoules were submerged in liquid nitrogen, and then subjected to vacuum in order to remove oxygen (which acts as a radical inhibitor). Direct vacuum was removed after a ten minute period, and the ampoules were thawed so that any trapped air bubbles could escape. The process of freezing and thawing was repeated twice (for a total of three freeze/thaw cycles) in order to ensure complete removal of oxygen. The ampoules were then sealed. Sealed ampoules were either stored in a freezer (-10°C)

ampoules were then sealed. Sealed ampoules were either stored in a freezer (-10°C) if they were to be used within one hour of being prepared, or stored in liquid nitrogen when storage beyond an hour was required.

Solutions of four individual compositions were prepared. They are illustrated in Table 3.2.3.1 below.

Table 3.2.3.1

Polymerization Runs

Solution #	Reaction Temperature (°C)	MMA : α-ms (weight ratio)	Trigonox B (weight %)
1	100	80:20	2
2	100	90:10	2
3	120	80:20	0.25
4	120	90:10	0.25

Evidence that the purification procedure effectively removed oxygen and other radical inhibitors is provided by the experimental conversion data. The presence of radical inhibitors would result in an induction period (that is, a period at the beginning of the reaction where no conversion would be observed). No induction period was observed.

3.3 Polymerization Reaction Runs

Temperature control was achieved using a silicon oil bath that was able to control temperatures to within ± 0.1°C for the temperature range in this study (100 - 120°C). The ampoules were submerged in the oil and were removed from the bath at time intervals such that a roughly 10 wt% conversion increase was observed between samples.

then opened and the contents were transferred to a 250 mL Erlenmeyer flask. At low conversion levels (< 20%), the ampoule contents remained fluid and were easily transferred to the flask. At intermediate conversion levels (20 - 60%), small quantities of the solvent tetrahydrofuran (THF) were used to facilitate the transfer of the ampoule contents to the flask. At higher conversion levels (>60%), the ampoule contents were usually solid enough that a small piece of the entire sample could be sliced off and transferred to the flask. The contents of the flask were then dissolved in approximately 20 mL of acetone (at low conversion) or THF (at intermediate and high conversion levels). In order to speed the dissolution of high conversion samples, the flasks were filled with 200 mL of THF and were stoppered until the samples dissolved (1 - 10 days). Minute quantities (less than 0.01g) of hydroquinone inhibitor were added to the high conversion samples to prevent any further polymerization. Once dissolved, the THF was allowed to evaporate until roughly 20 mL remained. Precipitation of polymer was accomplished by the addition of hexanes to the flasks. The flasks were then placed in a freezer (-10°C) for 48 hours to complete the precipitation process. The contents of the flask were filtered through medium porosity fritted glass filters, and both the flasks and filters were dried in a vacuum oven at 35-40°C for 4 days. The dried flasks and filters were removed from the oven, weighed, and put back in the oven after 3 days. No significant weight changes were observed when the samples were removed and weighed on the fourth day.

3.4 Product Characterization

The polymer products from the experiments were analyzed to determine conversion levels, composition, and molecular weight characteristics.

3.4.1 Gravimetric Analysis

The percentage of monomer converted to polymer was determined by gravimetric analysis. The equation below was used to calculate the conversion:

Conversion (mass fraction) =

(3.4.1.1)

$$\frac{\begin{array}{c}\text{mass of polymer and flask - mass of empty flask} \\ \text{+ mass of polymer and filter - mass of empty filter}\end{array}}{\text{mass of ampoule and reaction mixture - mass of empty ampoule}} \times (1 - \text{mass fraction of monomer in feed})$$

3.4.2 Composition

Polymer composition was obtained by proton nuclear magnetic resonance (^{1}H-NMR). The acquisition of NMR spectra was performed on a Bruker AMX500 ^{1}H-NMR under the following conditions:

deuterated chloroform (chloroform-D) as reference and solvent
spectrometer frequency of 500 MHz
relaxation energy of 0.01 seconds
pulse of 3 microseconds
acquisition time of 4.65 seconds
16 scans per readout (for averaging)
time domain of 65536 points
spectral window of 7042.25 Hz

Sample solutions were prepared for NMR analysis by dissolving each polymer sample in deuterated chloroform to yield 2 % w/v solutions. The spectral peak for MMA, corresponding to the OCH_3 grouping, was taken as the sum of the peaks in the 3.0 – 3.7 ppm range. The spectral peak for α-ms, corresponding to the benzene ring, was taken as the peak at roughly 7.2 ppm. A sample spectrum is shown in Figure 3.1.

The copolymer composition was calculated from the integrated spectral speak data as follows:

$$F_{MMA} = \frac{\frac{MMA\ Area}{3}}{\frac{MMA\ Area}{3} + \frac{\alpha - ms\ Area}{5}} \qquad (3.4.2.1)$$

and

$$F_{\alpha-ms} = \frac{\frac{\alpha - ms\ Area}{5}}{\frac{MMA\ Area}{3} + \frac{\alpha - ms\ Area}{5}} \qquad (3.4.2.2)$$

Division by three for the MMA peaks is necessary because the peak area is proportional to each of the three hydrogen atoms in the OCH_3 grouping. Similarly, division by five for the α-ms peaks is necessary because the peak area is proportional to each of the five hydrogen atoms on the benzene ring in α-ms.

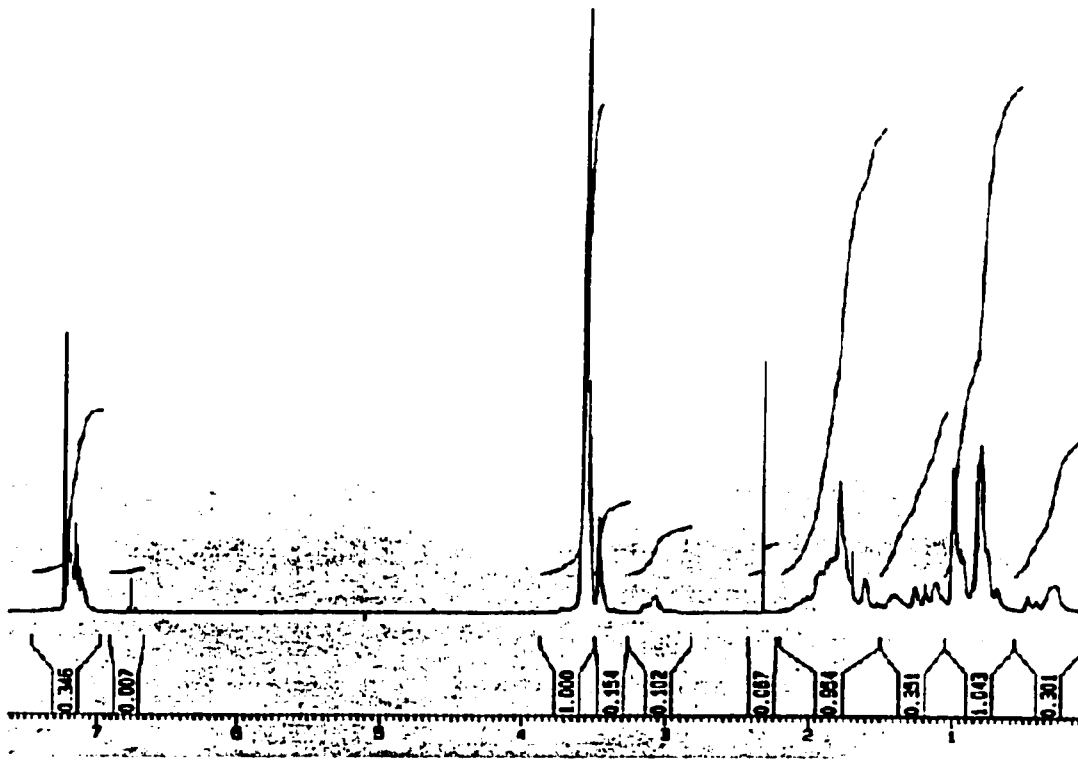

Figure 3.4.2.1 ^{1}H-NMR spectrum for an MMA/α-ms copolymer

3.4.3 Molecular Weight

Gel permeation chromatography (GPC) was used to obtain the number-average and weight-average molecular weights ($\overline{M}_n$ and $\overline{M}_w$) of polymer samples. The GPC components were as follows:

- Rheodyne 7725I injector
- Waters 610 fluid unit (pump)
- Waters Syragel column container with HR6, HR4 and HR3 columns, installed in series in that order
- Waters 600 pump controller
- Waters 410 differential refractometer
- Digital Venturis 575 Personal Computer
- Millennium 32 version 3.05 chromatography manager software
- HPLC grade tetrahydrofuran from VWR Canlab Inc. as the carrier fluid

Polymer samples were dissolved in 10 mL of tetrahydrofuran to produce solutions with concentration of 0.001 – 0.002 g / 10 mL. 200μL of each solution was injected with the Rheodyne injector. Flow rate through the column was maintained at 0.3 mL/min. Data were acquired for a period of 60 minutes after each injection was performed. The raw data were analyzed by Millenium 32 software in order to obtain the number-average and weight-average molecular weights of the polymers.

Modeling in Java™

At the time of publishing this thesis, the Java™ programming language had only been available to the public for a little over 3 years (Java 1.0 was released on January 23, 1996). As a result, to the best of this author's knowledge, this is the first published use of the Java language for developing a polymerization simulation package. This chapter will introduce the language, examine its merits and shortcomings, and discuss the suitability of the language for developing a polymerization simulation.

4.1 What is Java?

Java is a programming language developed by Sun Microsystems. Java was modeled after C++, which is a commonly used programming language. However, Java was designed to be less complex to program than C++ while retaining most of the language's powerful features.

What sets Java apart from most other programming languages, including C++, is that Java is designed to run programs on multiple platforms (i.e., multiple hardware / operating system combinations). In other words, a compiled Java program can run on different types of computers, be they Intel PC's, MacIntosh computers, or Solaris workstations (a full listing of Java compiler availability is provided in Appendix C). Java programs are able to do this because they are compiled in a different way.

With a traditional programming language, programs are compiled in one step, as illustrated below:

source code ⟶ *excutable*

With this scheme, one writes a program (source code), and uses a compiler program to convert the source code into an executable file. The executable file is used to run the program. Because the executable file contains platform-specific instructions, it can only be run on a single platform.

With Java, programs are compiled in two steps, as illustrated below:

$$\textit{source code} \longrightarrow \textit{bytecode} \longrightarrow \textit{interpreter}$$

With this scheme, one writes the source code and a Java compiler is used to convert the source code into Java bytecode. Bytecode files (which have the extension *.class*) contain program instructions that run on a "Java virtual machine". This virtual machine is not a physical piece of hardware, but rather it is akin to a microprocessor that is implemented in software. In order to run a Java program, a software "interpreter" program is used to emulate a Java virtual machine. By taking this approach, a single compiled Java program will run on any platform for which a Java interpreter is available.

4.2 Disadvantages of Programming in Java

Although Java has many features that are desirable for software developers, there are some disadvantages to using the language. Perhaps the most serious for numerical simulation development is speed, which may be unacceptably low for some numerical applications. Another consideration is that the language is new and any long-term project may require considerable modifications to work with the latest releases of the Java language. These disadvantages are discussed next.

4.2.1 Performance

For the purposes of developing a numerical simulation, Java has one significant disadvantage: speed. The process of interpreting Java bytecode requires

processor power. For applications where high performance is not a concern, Java's performance is usually more than adequate. However, for numerical simulations, an interpreted Java program may take up to 10 times more execution time than a similar program compiled in C++ . Such a performance penalty is likely too great to allow Java to be a serious option for developing numerical simulations. Fortunately, efforts have been made to eliminate the performance penalties arising from Java's interpreted nature. Just-In-Time compilers exist for several platforms. Just-In-Time compilers can achieve performance that is very near to natively compiled programs by compiling a Java program into native machine code as the program is running. This results in performance gains that are especially helpful for numerical simulations which, in general, contain a large number of repetitive 'loop' statements. Rather than having an interpreter convert a loop into native machine code every time the loop is repeated, a Just-In-Time compiler does this conversion only once. Every subsequent execution of the statements within the loop is done at optimum speed. As a result, Java's performance for numerical simulations can approach that of C++.

In addition to Just-In-Time compilers, compilers exist for several platforms that will compile Java programs into native machine code (i.e., executable files). While this may provide the highest speed of execution, an executable file will only function on a single platform, as is the case with other languages. In addition, such compilers may produce somewhat different numerical results than interpreted versions. The reason for possible differences is that there may be differences in the behaviors of the two compilers. For instance, all Java interpreters will perform rounding operations in the same way, applying IEEE 754 rules for numerical rounding operations (Gosling *et al.*, 1996). Compilers that generate executable files ideally would apply the same standards. In practice, however, there is no guarantee that such compilers will generate programs that behave identically to interpreted versions.

One unfortunate disadvantage to using an interpreter is in the debugging process. When using a debugger, a software tool designed to aid in locating and eliminating errors in a program, it is not possible to use a Just-In-Time compiler. As a result, the full performance penalty of using an interpreter is incurred when using a

debugger. A program that would normally take 1 minute to execute might take up to 10 minutes to execute in a debugger. Thus, for lengthy simulations, using other languages may be more practical than using Java.

4.2.2 Java is New and Evolving

Another practical consideration is that Java is still a relatively new language. As such, the language is still evolving. Although the actual syntax of the language has changed very little from the first release, the implementation of some language features has changed. Perhaps the single biggest change was that of the event models (the way events such as mouse clicks or key presses are handled by the language) used in versions 1.0x versus 1.1. While the new event model has substantial advantages over the old one, programs using the old event model required considerable modifications to use the new model. While a Java developer is never forced to use a newer version of the language, adopting newer versions may require considerable effort.

Finally, one must also consider that the development tools for Java are also in the process of evolving, just as the language is evolving. Although some excellent development tools are now available, some development tools available for other languages are undoubtedly more mature.

4.3 Advantages of Programming in Java

While developing software in Java does have the disadvantages discussed in the previous section, there are many advantages to developing software in Java. Java's platform-independent design makes porting Java programs to different operating systems a nearly effortless process. In addition, Java offers object-oriented design, graphical interface development, and is extensible and relatively simple, providing compelling reasons to choose Java for many programming needs. These advantages to developing programs in Java are discussed next.

4.3.1 Platform Independence

Thanks to its platform-independent design, Java allows developers to write programs that will run on all major operating systems without modification or even recompilation. Java offers developers easy access to powerful windowing and networking features through the Java API (Application Programming Interface), a standard code library that is guaranteed to be available on all Java-compatible platforms. Although other languages may have a certain degree of standardization that aids in cross-platform development, only Java offers one universally available API for all operating system platforms.

4.3.2 Object-Oriented

Java is an object-oriented language. Object-oriented programs are highly structured so that they are simpler to understand than procedural programs, and program code is more easily modified and reused. For model-based simulation programs, object-oriented programming allows the structure of the program to reflect the structure of real-world systems.

The implementation of the object-oriented structure in Java is efficient, even for numerical simulations. Since primitive data types (e.g., integer and floating-point numbers) are *not* implemented as objects, calculations do not suffer the speed and overhead penalties of using objects for primitive data types. It should be noted that object equivalents exist for each of the primitive data types to cover situations where they might be useful.

4.3.3 Java is Multithreaded

Java, like the programming language Ada, but unlike other languages, provides built-in support for multithreading. Multithreading allows more than one "thread" of execution to take place on a single processor. The result is that a program

will appear to do several tasks simultaneously. For example, a Java program could do calculations, update a graph, and accept user input all seemingly at the same time. Multithreading support means that it is possible to write multithreaded programs while still maintaining a high degree of reliability. Program activities can be synchronized, thereby eliminating undesired and potentially disastrous interactions between different threads of execution.

4.3.4 Simplified Syntax and Program Design

As was mentioned in the introductory remarks of this chapter, Java was modeled after C++. However, Java was designed to make the software development process simpler and less error-prone than C++. Java makes programs simpler by eliminating the header files used in C++. Java simplifies the process of making API calls by importing the required API software packages. Java eliminates the more error-prone features of C++, such as automatic data type conversion. In C++, the compiler will convert data from one type to another without issuing a warning. In Java, the programmer must explicitly cast one data type to another to indicate that he or she understands that a conversion (and possibly an alteration of data) may occur. Java eliminates the need for pointers, and thus, complex pointer arithmetic, making the language simpler. Also, Java has automatic memory management. Objects in memory that can no longer be referenced are automatically cleared from memory by Java's "garbage collection" feature. Java does not require programmers to write the "destructor" methods that are required in C++.

4.3.5 Support for Arbitrary Precision Numbers

Java's built-in primitive for double precision numbers is 64-bits long (IEEE 754 standard). For most purposes, 64-bits is sufficient. However, for situations where 64-bits is not sufficient, Java versions 1.1 and higher support arbitrary precision numbers. Thus, precision-sensitive calculations, such as dividing by the difference between two similar values, can be done at arbitrarily chosen higher

precision levels (e.g., 128-bits). This feature may be invaluable for certain simulations; however, its use incurs a considerable speed penalty, which increases as the desired precision increases. Thus, it is advisable to use this feature sparingly.

4.3.6 Ease of Documentation

One of the main advantages of object-oriented languages is code reuse. Java encourages code reuse not only by its object-oriented nature, but also by providing a means to easily create documentation for software written in Java. The javadoc utility, a program that is included in the free Java Developers Kit (jdk) from Sun Microsystems, automates the process of software documentation. If specially formatted comments (delimited by the characters /** and **/) are inserted into source code, the javadoc utility can extract the comments and use that information to generate professional-looking documentation. The documentation is presented in HTML-document format, similar to Web pages, and features links to related sections of documentation. This makes it extraordinarily easy to navigate through the documentation to find desired information.

Due to the fact that the comments for the documentation are included in the source code files, it is very simple to keep the documentation current. Whenever a modification is made to the source code, the nearby comments are simply altered to reflect any changes. Using the javadoc utility with the altered source file creates up-to-date documentation.

4.4 Was Java Found to be Appropriate?

In terms of the development of the polymerization simulation program, the most important disadvantage of using Java was found to be the slow execution of the program during debugging. While the program would normally require 2 to 10 seconds to run a simulation when employing a Just-In-Time compiler to run the program, it would take roughly ten times longer to run the same simulation in the

debugger. This speed penalty during debugging did not significantly impede the development of the simulation program, but would definitely be a major concern for programs that require longer execution times.

The simplified language syntax and object-oriented structure of the Java programming language were the main features that influenced the decision to choose Java to develop the simulation. These features allowed the development of a highly structured program with a minimum amount of difficulty.

Since the disadvantages of using Java did not significantly impede the development of the simulation, and the simulation program was successfully developed with a reasonable amount of effort, Java was found to be appropriate for the development of the polymerization simulation program.

4.5 When is Java appropriate?

As discussed above, developing programs in Java has both advantages and disadvantages. With these advantages and disadvantages in mind, one may attempt to answer the question of when the use of Java is appropriate in general. Due to possible speed penalties when using Java, C++ is usually the language of choice for developing programs that require both absolute performance and a graphical user interface. On the other hand, FORTRAN is the language of choice for the most complex and calculation-intensive software development (e.g., those where a super-computer is used). For most other programming needs, Java appears to be an excellent choice.

4.6 Program Behavior

A user is able to run the simulation program by executing Frame1.class (if a Java compiler is used), or by running an executable file named Impress.exe (currently

available for Windows95/98). An introductory screen is shown briefly as the program loads. Once the program has loaded, the user is shown a screen similar to the following:

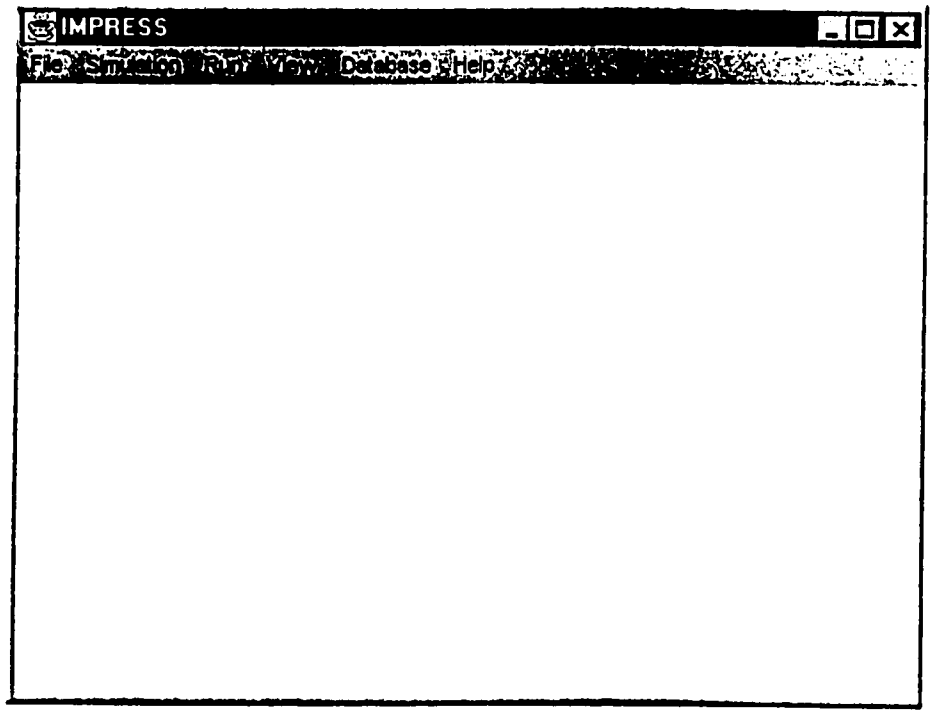

Figure 4.6.1 Main program screen

The user can chose the system to be simulated by selecting the Simulation menu (by clicking the mouse on the word Simulation), and choosing the Edit Run Conditions menu item that will appear when the Simulation menu is selected. A dialog box will appear that allows the user to choose the system to be simulated as well as options for what simulation results will be saved to a file. The dialog box has 6 tab panels that allow the user to customize simulation behavior. The first tab panel, Reaction Conditions, is shown in Figure 4.6.2. The Reaction Conditions tab panel has interface components that allow the user to set the amount of reaction time to be simulated and the conversion limit for the reaction. The program will continue to simulate a reaction until the user-inputted reaction time limit has been reached, or the

conversion limit has been reached (whichever occurs first). This tab also allows the user to set the temperature at which the simulated reaction is to proceed.

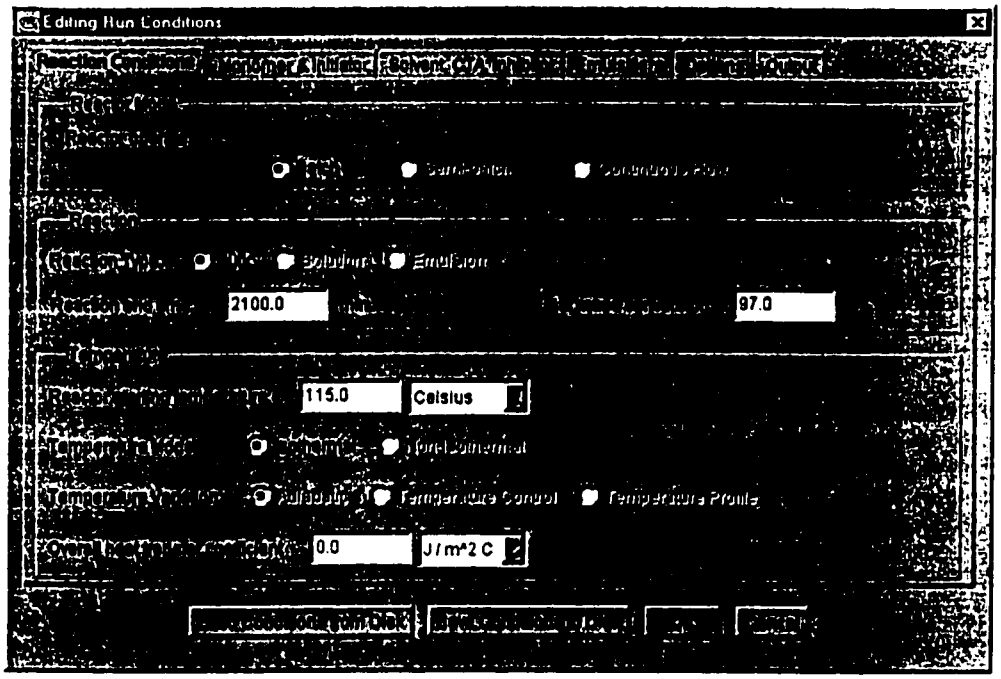

Figure 4.6.2 Editing Run Conditions Dialog – Reaction Conditions tab

The Monomer & Initiator tab panel, shown in Figure 4.6.3, allows the user to select both the amount and type of monomers and initiator to be present in the simulated reaction medium. The Solvent, CTA, Inhibitor tab panels serves a similar purpose, allowing the user to select the amount and type of solvent, chain transfer agent, and inhibitor to be present. The Emulsifiers tab panel is not functional and currently serves only as a placeholder for future program development since the program is not yet equipped to simulate emulsion polymerization reactions.

The Options tab panel, shown in Figure 4.6.4, allows the user to customize model behavior. Using this tab, the user can enable or disable the inclusion of: diffusion-control, depropagation, thermal initiation and variable initiator efficiency effects in the simulation. The tab also allows the user to select a numerical tolerance parameter as a value between 4 and 8 inclusively. The numerical tolerance parameter determines the accuracy of the differential equation solver calculations. Choosing

higher values for the numerical tolerance parameter causes the differential equation solver to produce more accurate results at the expense of longer program execution.

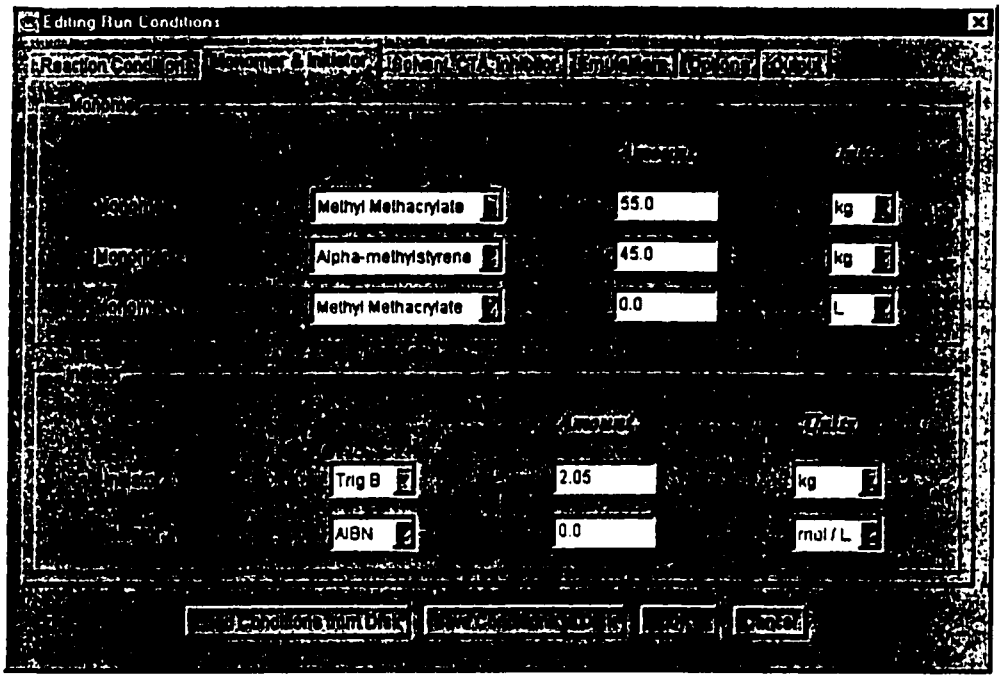

Figure 4.6.3 Editing Run Conditions Dialog – Monomer & Initiator tab

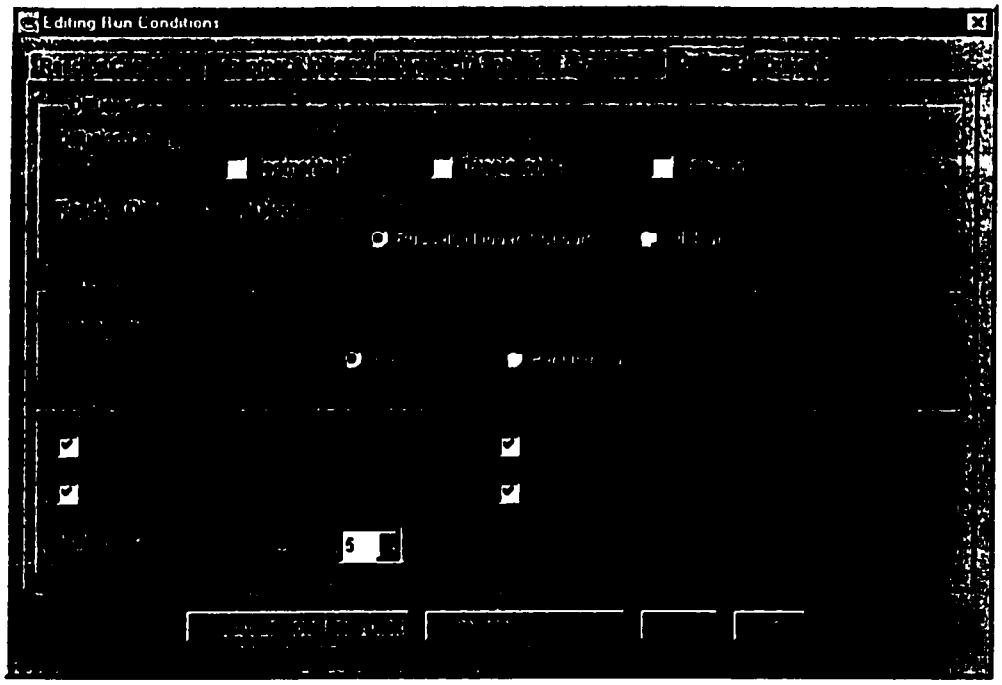

Figure 4.6.4 Editing Run Conditions Dialog – Options tab

Finally, the Output tab panel, shown in Figure 4.6.5, allows the user to select the simulation data to be placed in an output file (named output.txt).

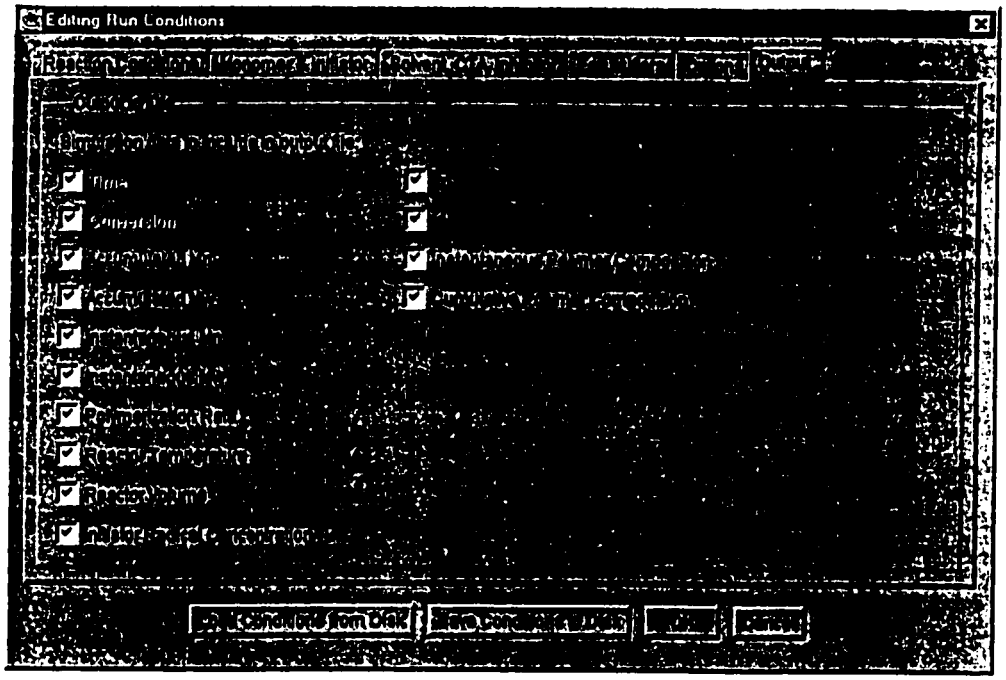

Figure 4.6.5 Editing Run Conditions Dialog – Output tab

4.7 Program Validation

Like any object-oriented program, the simulator is divided into several classes, each serving a rather specific purpose. The classes can largely be divided into four categories: classes that relate to the user interface, classes that relate to the database, classes that relate to the mathematical solution of the polymerization model, and classes that relate to the polymerization model.

Verifying the proper function of the user interface classes was a straightforward process. The user interface can be visually inspected to be functioning properly by running the program and using the interface.

Testing the database classes was also a straightforward process. The contents of the database were examined and verified to contain the proper data in the correct order.

The differential equation solver used in the program is that described in chapter 16.6 of the book Numerical Recipes in C (Press *et al.*, 1992). The solver was translated from C into Java, and divided into several classes. The solver was tested against the example of a system of stiff differential equations shown in the book, as well as some other systems of differential equations for which analytical solutions could easily be derived, and was found to function correctly.

Testing the model classes was the most difficult process. Because it is not feasible to develop an analytical solution to the model (due to the complexity of the complete model), it is not possible to verify the model classes simply by comparing program predictions with an analytical solution except in the simplest cases. An example of a case that can be solved analytically is presented in Appendix D. For such simple cases, the program was found to match analytical solutions with the expected degree of accuracy (in accordance with the value chosen for the numerical tolerance parameter). For the more complex cases, the Java program's output was compared to published data in Gao and Penlidis (1996, 1998). Since Gao and Penlidis used a similar model to generate their simulation data, and their simulator has been tested against a broad range of experimental data, agreement with their simulation data is a good indication that the Java program yields good predictions. As will be discussed in the next chapter, agreement between the simulation data from the Java program and the results published by Gao and Penlidis was consistently good.

Results and Discussion

The focus of this thesis was to develop a simulation program which could model copolymerization systems that exhibit significant depropagation effects. The model used is mechanistic in nature and is thus more general than an empirical model. As a result, the model is applicable to a large number of polymerization systems under a wide variety of conditions. The program's predictions were compared with data for both homopolymer and copolymer systems where depropagation effects could be ignored. Once the program was established to be functioning correctly for non-depropagating systems, the incorporation of depropagation effects into the program and comparisons of the program's predictions to experimental results were carried out.

5.1 Homopolymerization of α-methylstyrene

α-methylstyrene is a monomer that is known to undergo depropagation at relatively low temperatures. The ceiling temperature of α-methylstyrene is just 61°C (Wittmer, 1971). Thus, polymer can only be formed at temperatures below 61°C. However, at such temperatures, free-radical polymerization rates for α-methylstyrene are extremely low. In fact, it would take weeks to get appreciable conversion, unless one adds so much initiator that only very low molecular weight material would be formed ($\overline{M}_w < 5000$). This explains why there appears to be no data in the literature on the free-radical homopolymerization of α-methylstyrene – it would be impractical to produce this polymer using free-radical polymerization.

It should be noted that the polymerization of α-methylstyrene by anionic polymerization has been studied. The interested reader is referred to Zhuang *et al.* (1997) for further information. Since the program's model is not equipped to handle anionic polymerization, and no data are available for comparison of free-radical homopolymerization predictions, no model comparisons to experimental homopolymerization data can be made.

5.2 Homopolymerization of Methyl Methacrylate (MMA)

Model predictions for methyl methacrylate in the temperature range of 50°C - 90°C have been established to be very good. Gao and Penlidis (1996) present results for their simulation of bulk polymerization of methyl methacrylate with 2,2'-azobis(isobutyronitrile) (AIBN) as the initiator in the 50°C - 90°C temperature range. Their results were found to match experimental data very well. The results of the simulation using the Java program that was written for this study, which uses a similar model, also match the experimental and simulation data very well. An example plot showing experimental results published in Gao and Penlidis (1996) and predictions from the program developed for this thesis is shown in Figure 5.2.1 below.

Gao and Penlidis (1996) provided an extensive amount of experimental data for MMA homopolymer over the 50-90°C temperature range and used a variety of initiators and chain transfer agents. The simulator developed for this thesis was tested against the large amount of experimental data for bulk MMA homopolymerization when AIBN or dimethyl 2,2'-azobisisobutyrate (AIBME) was used as initiator, and n-dodecyl mercaptan as chain transfer agent, and was found to match the experimental data very well in almost all cases.

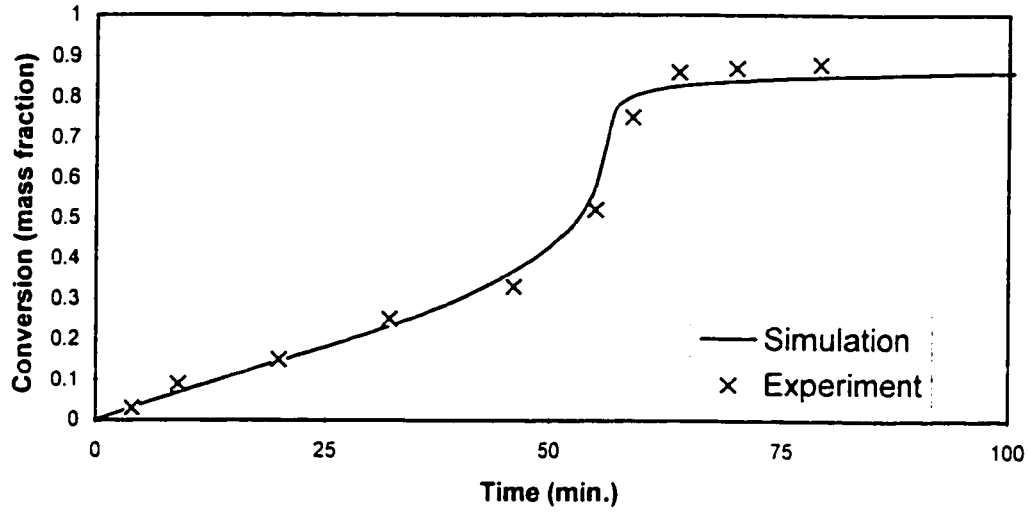

Figure 5.2.1 Conversion vs. time plot for bulk reaction of MMA at 50°C, [AIBN] = 0.0248 mol/L

The simulation predictions shown in Figure 5.2.1 do not include the effects of depropagation, and yet the predictions are quite good. The reason that the inclusion of depropagation effects was not required to achieve accurate predictions is that depropagation effects are negligible at lower temperatures. As can be seen in Figure 5.2.2, the effects of depropagation on the polymerization of methyl methacrylate are essentially negligible below 90°C. In other words, it is thermodynamically possible to achieve essentially 100% conversion of monomer into polymer below 90°C. Above 100°C, the effects of depropagation begin to manifest themselves as the limiting conversion begins to decrease. However, even at 140°C (the highest temperature examined in this study), it is thermodynamically possible to achieve roughly 95% conversion.

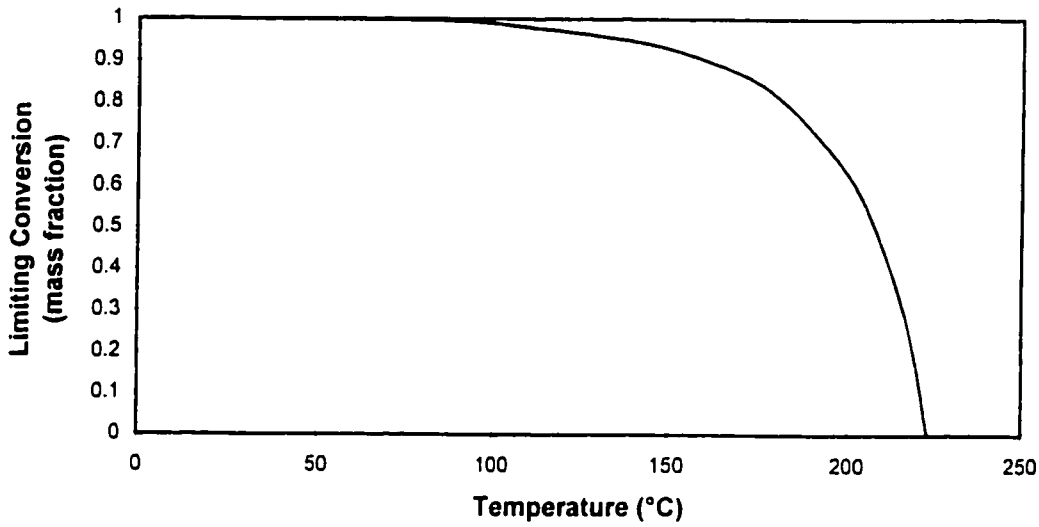

Figure 5.2.2 Limiting conversion versus temperature for methyl methacrylate, based on predictions from the simulation program.

Data for the value of the equilibrium constant K, defined in equation 2.8.3, were required to generate Figure 5.2.2. An Arrhenius type expression of the form

$$K = A\exp(-E_a / RT)$$

was fitted to data for K that was obtained from Wittmer (1971). Wittmer's data are plotted along with the curve-fit data in Figure 5.2.3. As can be seen in Figure 5.2.3, the Arrhenius curve-fit appears to be an appropriate model for the data. Furthermore, a plot of the residuals did not indicate any reason to question the appropriateness of the proposed Arrhenius fit. An Arrhenius model is reasonable for K since it is defined as the ratio of two reaction rate constants, each of which can be expressed in terms of an Arrhenius expression.

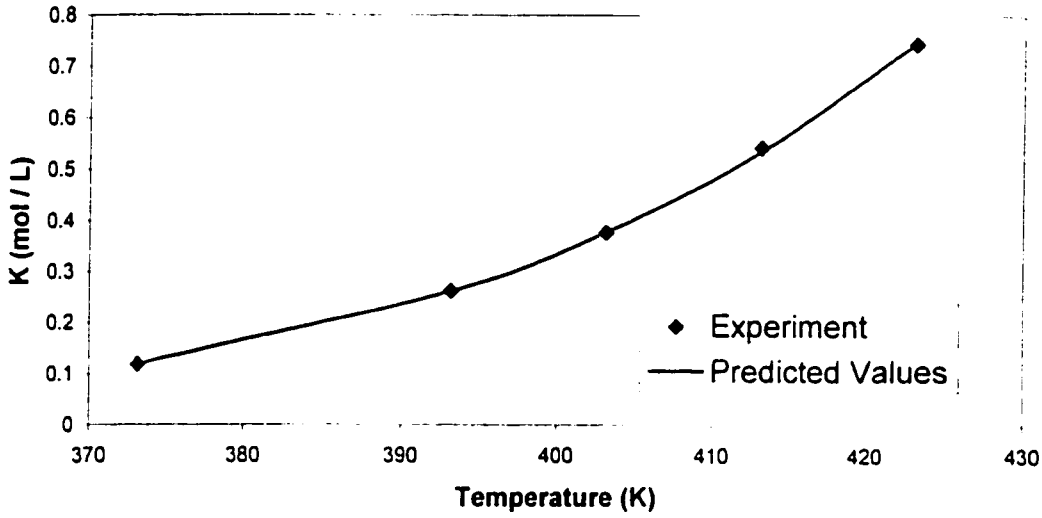

Figure 5.2.3 Curve-fit of Wittmer's experimental *K* data for methyl methacrylate

Using the data for *K*, the program was modified to predict the ceiling temperature. The program predicted a ceiling temperature of 232°C, whereas the literature value is reported as 220°C (Odian, 1991).

Simulation predictions and experimental data (from Dubé *et al.*, 1995) for conversion versus time at 115°C are shown in Figure 5.2.4. The agreement between simulation predictions and experimental results for conversion levels below 0.75 is quite good, with agreement being within ±0.05 of experimental data. However, above conversion levels of 0.75, much larger deviations between experimental data and simulation predictions are observed. It should be noted that the simulation predictions that include depropagation effects are nearly indistinguishable from predictions where depropagation effects have been ignored. Interestingly, equilibrium data indicate that the limiting conversion at 115°C is roughly 97.5%, yet the experimental results do not indicate that there is a limit to the conversion. This discrepancy is most likely due to a small amount of the solvent that was used to separate monomer from polymer being trapped in the polymer lattice. This is a common problem that is often most pronounced at high conversion (and higher molecular weight) levels. The weight of the trapped solvent is unintentionally added

to the measured weight of dried polymer during gravimetric analysis. As a result, the experimental conversion data are higher than they should be.

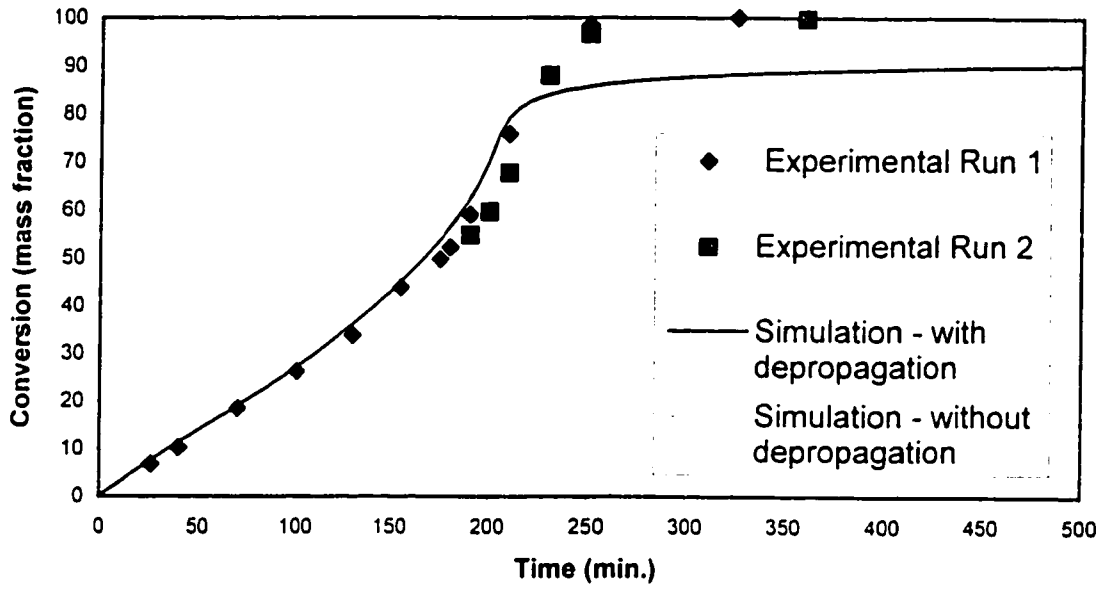

Figure 5.2.4 Conversion versus time at 115°C for methyl methacrylate. Trigonox B as initiator = 0.3 wt%, n-dodecyl mercaptan is CTA = 0.002 wt%. (Data from Dubé *et al.*, 1995)

Predictions of the cumulative weight-average molecular weight, $\overline{M}_w$, and cumulative number-average molecular weight, $\overline{M}_n$, at 115°C are shown in Figure 5.2.5. The predictions for $\overline{M}_w$ are within ±15% of the experimental data, while the $\overline{M}_n$ predictions are within ±40% of the experimental data. The agreement is reasonably good considering that molecular weight measurements are prone to errors.

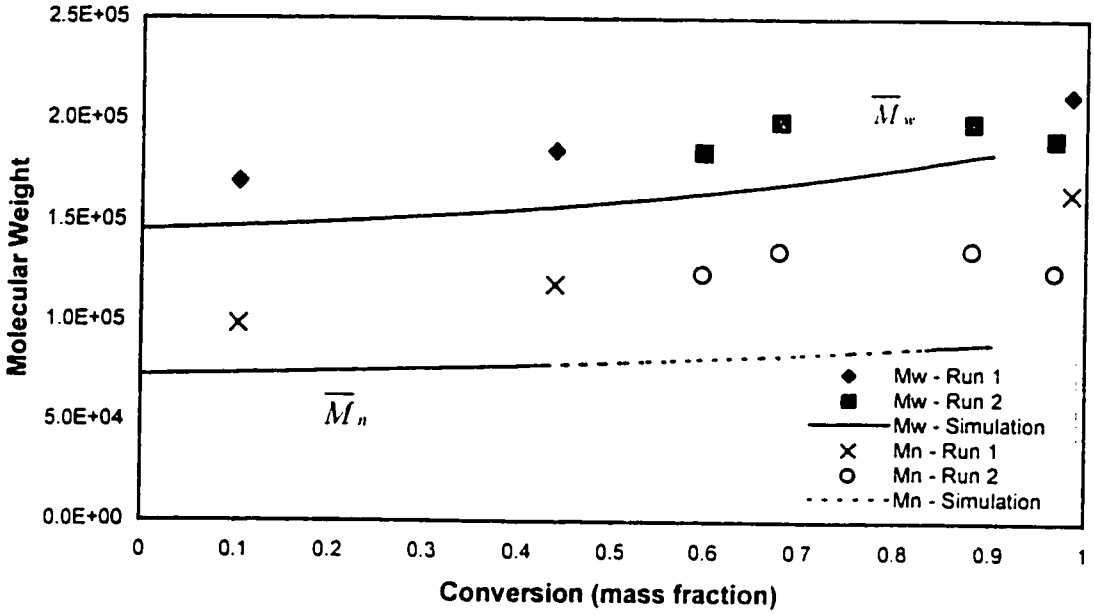

Figure 5.2.5 $\overline{M}_w$ and $\overline{M}_n$ versus time at 115°C for MMA. [Trigonox B] as initiator = 0.057 wt%. [n-dodecyl mercaptan] as chain transfer agent = 0.19 wt%. (Data from Dubé *et al.*, 1995)

5.3 Copolymerization without Depropagation Effects

The program is not only able to simulate homopolymerizations, but it can also be used simulate copolymerizations as well. As a first step, the program was written to handle copolymerizations that do not exhibit the effects of depropagation. The case of copolymerization without depropagation has received considerable attention in the literature and examining this case serves to verify the proper functioning of the program. A test case of the copolymerization of MMA and Styrene was chosen because the model parameters for both of these monomers are well established in the literature. A comparison of simulation results from the program and experimental results published in the comprehensive article on free-radical copolymerization by Gao and Penlidis (1998) is shown in Figure 5.3.1 below.

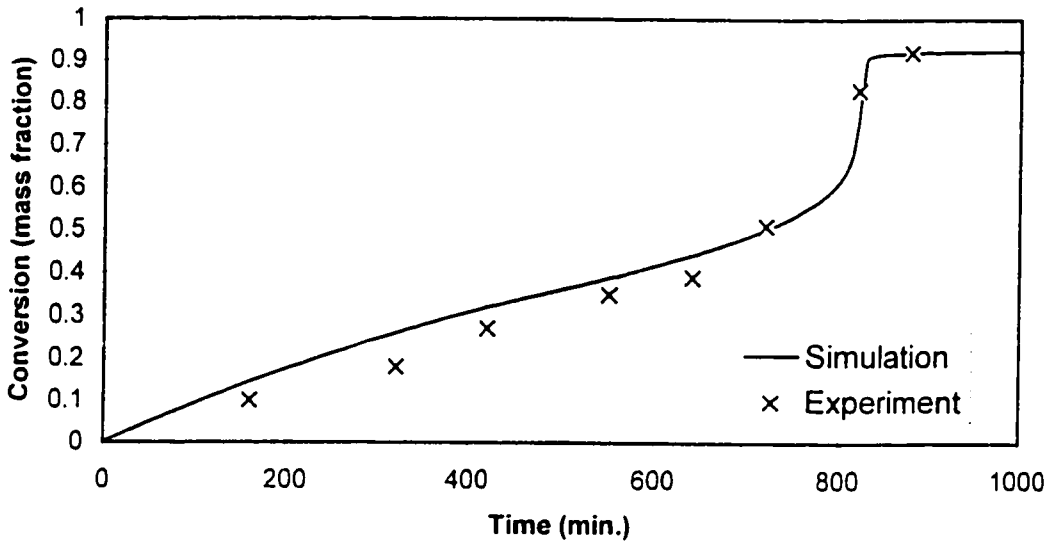

Figure 5.3.1 Conversion vs. time for MMA/Styrene copolymerization at 60°C. MMA:Styrene = 70:30 (molar ratio), [AIBME] (dimethyl 2,2'-azobisisobutyrate) as initiator = 0.01 mol/L. (Data from Gao and Penlidis, 1998)

As can be in Figure 5.3.1, agreement between simulation and experimental data is good, with conversion predictions being within ± 0.05 for nearly all the data. Similar agreement between simulation and experimental data was observed even when the initiator type and concentration, as well as monomer feed composition were varied (not shown).

The close correspondence of the simulation data generated by the Java program and the experimental and simulation data of Gao and Penlidis, in conjunction with the positive results from attempts to validate the simulator (as discussed previously), lead to the conclusion that the Java program functions correctly when simulating both homo and copolymerization reactions that do not exhibit significant depropagation effects.

5.4 Copolymerization with Depropagation Effects

Once it was established that the program was capable of simulating copolymer systems that do not exhibit depropagation effects, the program was extended to handle cases where depropagation effects could not be neglected. This is the first published use of a general mechanistic model to simulate the conversion, composition, and molecular weight profiles during free-radical copolymerization in cases where depropagation effects for both monomers cannot be ignored. Extension of the program to handle copolymerizations with depropagation was done by implementing the model described by Kruger *et al.* (1987). Kruger's method was chosen over the method of Wittmer (1971). Palmer (1999) showed that Kruger's method is numerically stable over the entire range of polymer compositions when applied to the MMA/α-ms system, whereas Wittmer's method is not. Palmer's estimates for the reactivity ratios, as well as parameters for Kruger's equations for the MMA/α-ms system, were used in the program. Note that Palmer used Kruger's model in conjunction with his own experimentally measured values of parameters to simulate polymer composition as a function of conversion, but did not attempt to use the model to simulate conversion or molecular weight as a function of time.

5.4.1 Copolymerization of MMA/α-ms at 100°C

The experimental results obtained during this study for conversion versus time at 100°C are shown along with simulation data in Figures 5.4.1.1 and 5.4.1.2 below. As can be seen in the figures, the simulation data for conversion versus time at 100°C follows the curvature of the experimental data, although experimental results show nearly 100% conversion being achieved whereas the simulation data indicate a definite limit to the maximum achievable conversion. These discrepancies between experimental results and simulation data at high conversion levels are similar to those obtained for MMA homopolymerization. The cause is likely the same in both cases:

the solvent used to separate monomer from polymer becomes trapped in the polymer lattice, particularly at high conversion levels.

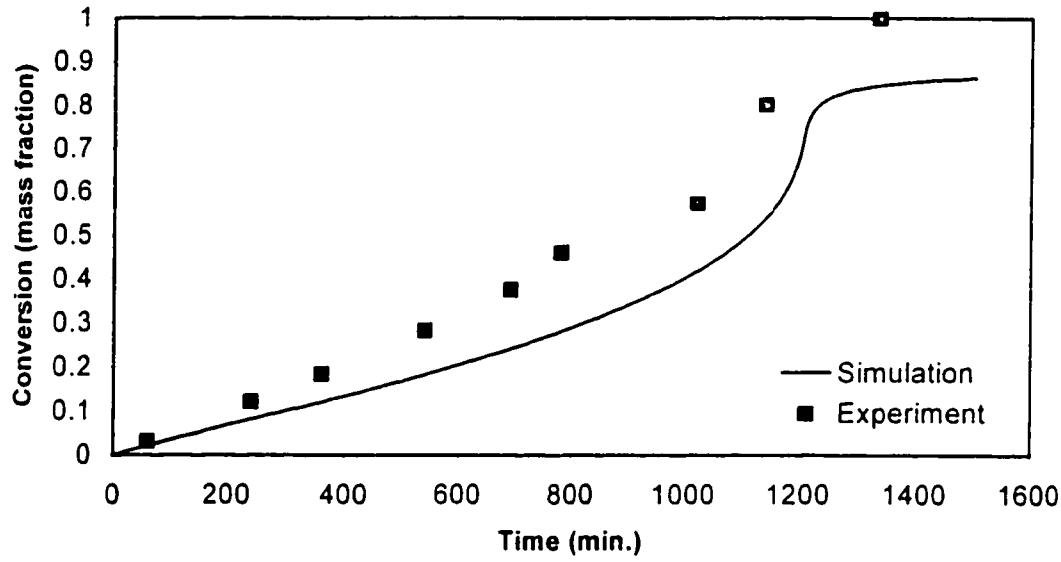

Figure 5.4.1.1 Conversion vs. time for MMA/α-ms copolymerization at 100°C. MMA:α-ms = 80:20 (weight ratio), [Trigonox B] as initiator = 2.0 wt%.

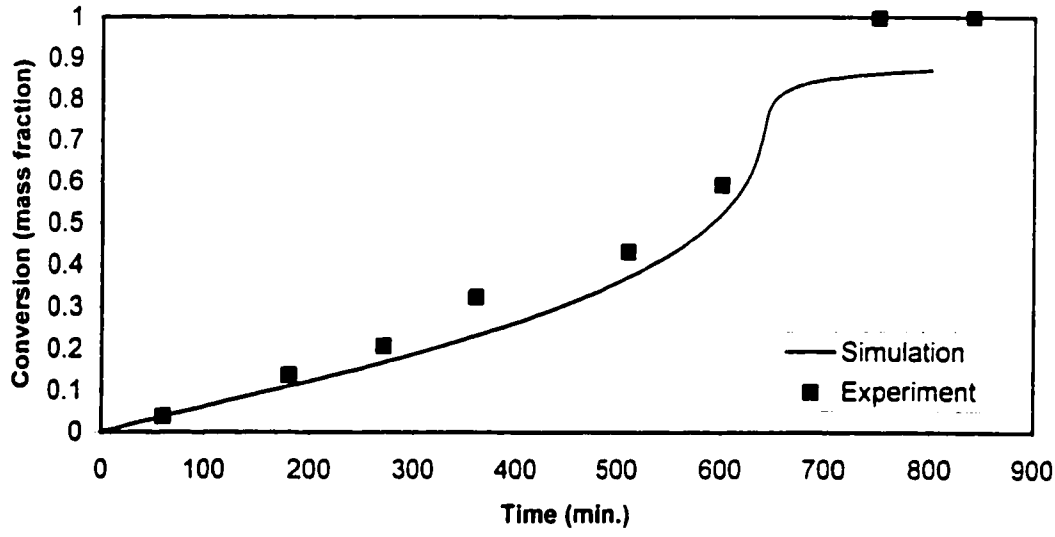

Figure 5.4.1.2 Conversion vs. time for MMA/α-ms copolymerization at 100°C. MMA:α-ms = 90:10 (weight ratio), [Trigonox B] as initiator = 2.0 wt%.

Experimental results for $\overline{M}_w$ versus time at 100°C are shown along with simulation data in Figures 5.4.1.3 and 5.4.1.4 below. As can be seen in the figures, the simulation data for $\overline{M}_w$ versus time at 100°C match experimental results closely, except at very high conversion levels. In fact, this is the only temperature level examined in this study for which simulation data for $\overline{M}_w$ match experimental results. This is likely due to one or both of two reasons. Firstly, many of the parameters that affect molecular weight, such as rate constants for chain transfer reactions, have been obtained at lower temperatures. The accuracy of extrapolating these parameters to the higher temperatures examined in this study is questionable, but is currently required due to the absence of high temperature data. Secondly, the model for molecular weight predictions was originally derived under the assumption that the propagation reaction is irreversible. The modifications that were made to that model in an attempt to account for depropagation may be inadequate, and perhaps an alternate method for molecular weight predictions should be sought.

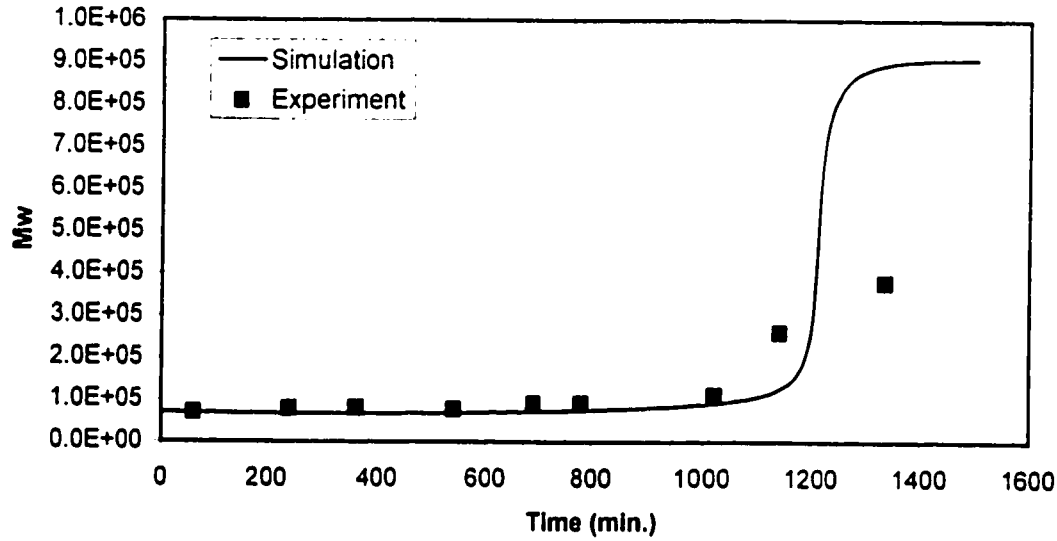

Figure 5.4.1.3 $\overline{M}_w$ versus time for MMA/α-ms copolymerization at 100°C. MMA:α-ms = 80:20 (weight ratio), [Trigonox B] as initiator = 2.0 wt%.

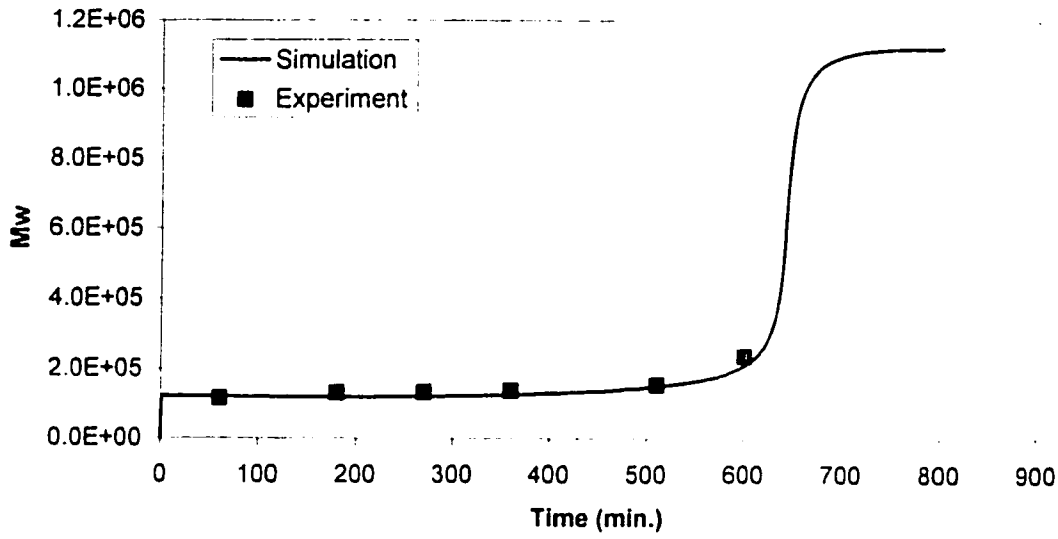

Figure 5.4.1.4 $\overline{M}_w$ versus time for MMA/α-ms copolymerization at 100°C. MMA:α-ms = 90:10 (weight ratio), [Trigonox B] as initiator = 2.0 wt%.

Experimental results for cumulative copolymer composition versus conversion at 100°C are shown along with simulation datas in Figures 5.4.1.5 and 5.4.1.6 below. As can be seen in the figures, the simulated data for cumulative copolymer composition versus conversion at 100°C are in close agreement with experimental data. In fact, simulation data for copolymer composition were found to closely match experimental data at all of the temperature levels examined in this study (100, 115, 120, and 140°C). In all of the cases examined, the experimental data indicate that the polymer composition for this copolymer system changes very little as a function of conversion.

It should be noted that the value of one of the parameters that affects copolymer composition, R_{AA} for MMA as defined in equation 15 in Appendix A, was estimated at 100, 115 and 120°C because no experimental data were available. Palmer (1999) reported an experimental value of R_{AA} = 1.4 at 140°C when measured in bulk, and a value of R_{AA} = 2.1 at 140°C when measured in solution, even though the value of the parameter should not be affected by the presence of solvent. Obviously, it was difficult to measure this parameter experimentally, particularly

because its value is related to the degree that MMA depropagates, which is quite low at or below 120°C. A value of $R_{4,4} = 2.1$ was used in simulations at 140°C because it yielded the best copolymer composition predictions. The value of $R_{4,4}$ was taken to be 0.5 at 100°C, 1.2 at 115°C, and 1.4 at 120°C so that the $R_{4,4}$ values would follow a similar trend to the equilibrium constant K for MMA, roughly doubling for every 20°C temperature increase.

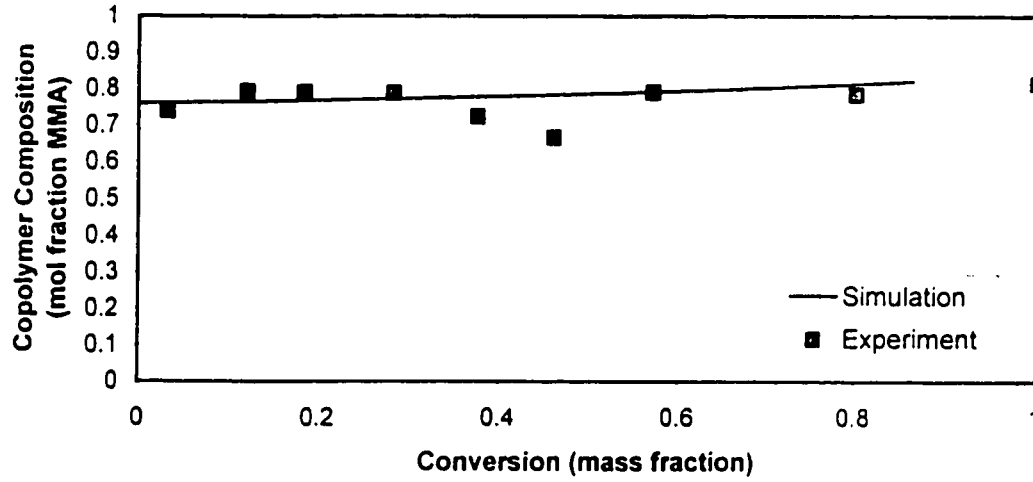

Figure 5.4.1.5 Copolymer composition versus conversion for MMA/α-ms copolymerization at 100°C. MMA:α-ms = 80:20 (weight ratio) , [Trigonox B] as initiator = 2.0 wt%.

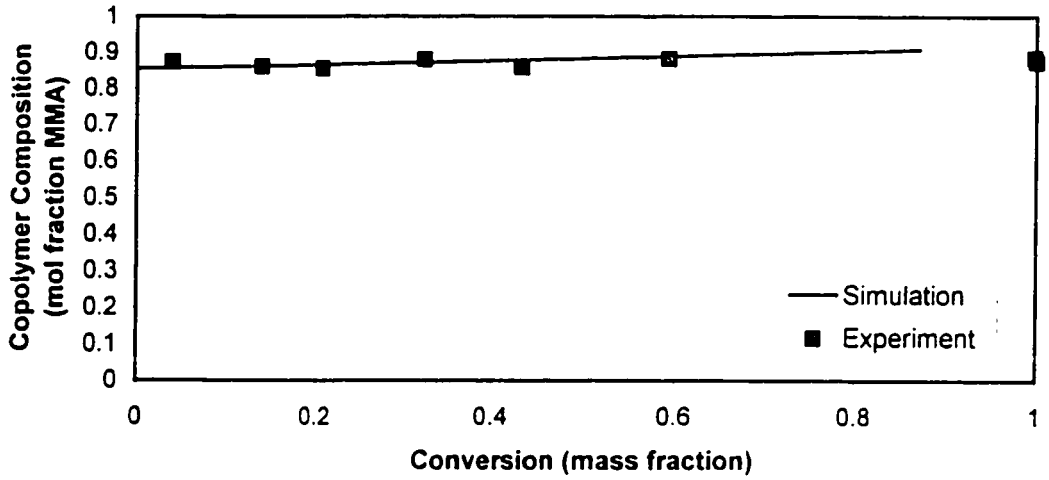

Figure 5.4.1.6 Copolymer composition versus conversion for MMA/α-ms copolymerization at 100°C. MMA:α-ms = 90:10 (weight ratio) , [Trigonox B] as initiator = 2.0 wt%.

5.4.2 Copolymerization of MMA/α-ms at 115°C

Experimental data for MMA/α-ms copolymerization at 115°C were obtained from Palmer (1999). Experimental results and simulation data for conversion versus time at 115°C are shown in Figures 5.4.2.1 and 5.4.2.2 below. As can be seen in the figures, the data follow the trends of the experimental data quite closely but are somewhat lower than experimental data at high conversions. This may again be due to solvent being trapped in the polymer, or it may be due to uncertainty in the value of the Kruger model parameter R_{AA} for MMA. It should also be noted that most of the deviations are within the limits of the experimental reproducibility of roughly ± 5% for the high conversion data that Palmer reports at 140°C. Although Palmer did not examine the reproducibility of his data at 115°C, it is likely to be very similar to the reproducibility at 140°C.

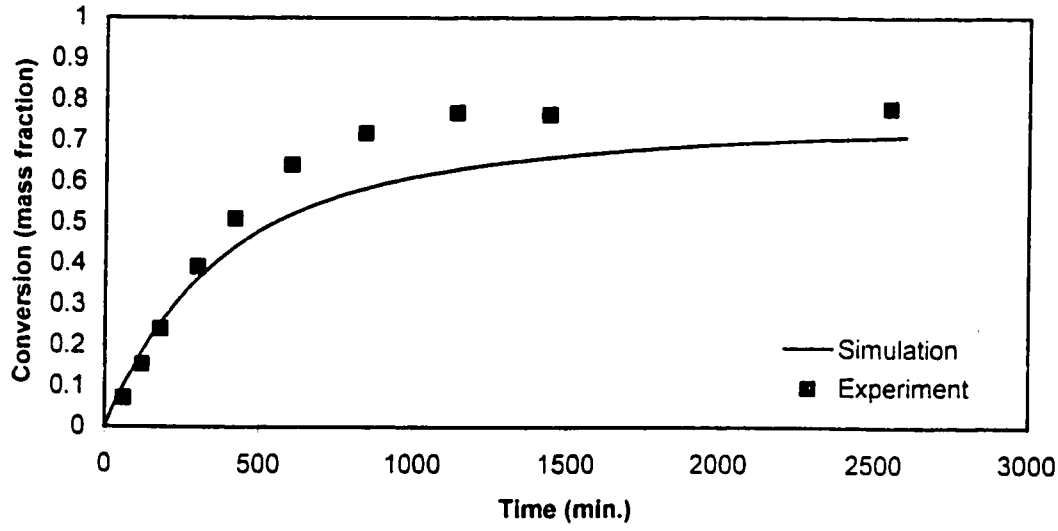

Figure 5.4.2.1 Conversion vs. time for MMA/α-ms copolymerization at 115°C. MMA:α-ms = 60:40 (weight ratio), [Trigonox B] as initiator = 4.0 wt%. (Data from Palmer, 1999)

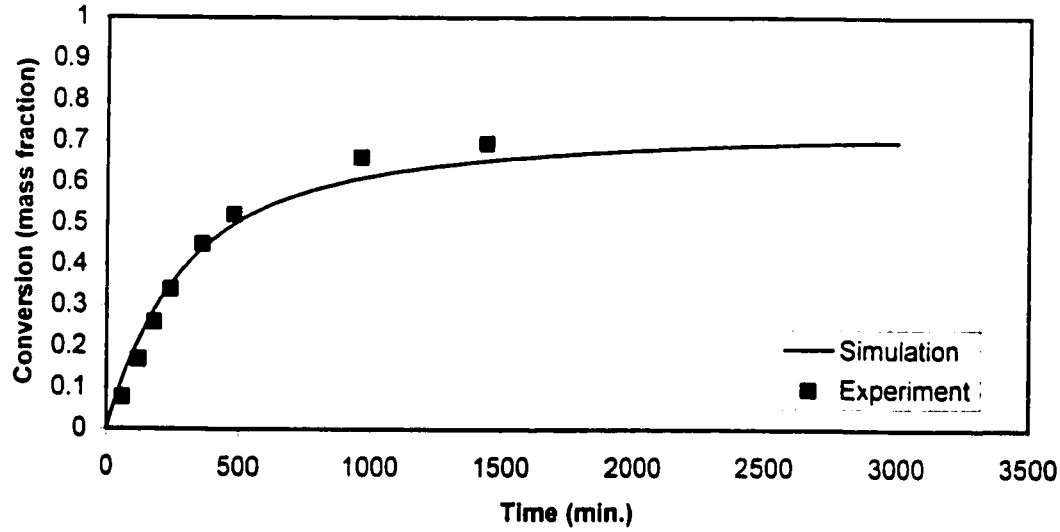

Figure 5.4.2.2 Conversion vs. time for MMA/α-ms copolymerization at 115°C. MMA:α-ms = 55:45 (weight ratio), [Trigonox B] as initiator = 8.0 wt%. (Data from Palmer, 1999)

It should also be noted that the simulation data at 115°C were prepared with diffusion-controlled termination effects disabled in the program options. This option had to be disabled in order to achieve good conversion versus time predictions. The shape of the conversion versus time graphs suggests that diffusion-controlled termination effects are negligible (an S-shaped curve would have suggested that they were significant). When the option was enabled, the program had computed that diffusion-control effects were significant and generated an S-shaped conversion versus time curve that did not match experimental results. One reason that this may have occurred is that $\overline{M}_w$ predictions, shown in Figures 5.4.2.3 and 5.4.2.4 below, were too high, particularly at low conversion. $\overline{M}_w$ predictions affect the calculation of diffusion-controlled termination effects in the program, as shown in section 2.9. If the predicted value of $\overline{M}_w$ is too high, significant diffusion-control effects will be calculated to occur before they would occur experimentally. Alternatively, the diffusion-control parameters for α-ms may not be very accurate, and this may have resulted in diffusion-control effects being determined to occur in the program when they do not occur experimentally.

Experimental and simulation data for cumulative copolymer composition versus conversion are shown in Figures 5.4.2.5 and 5.4.2.6 below. As can be seen in the figures, simulation data for cumulative copolymer composition closely match experimental data.

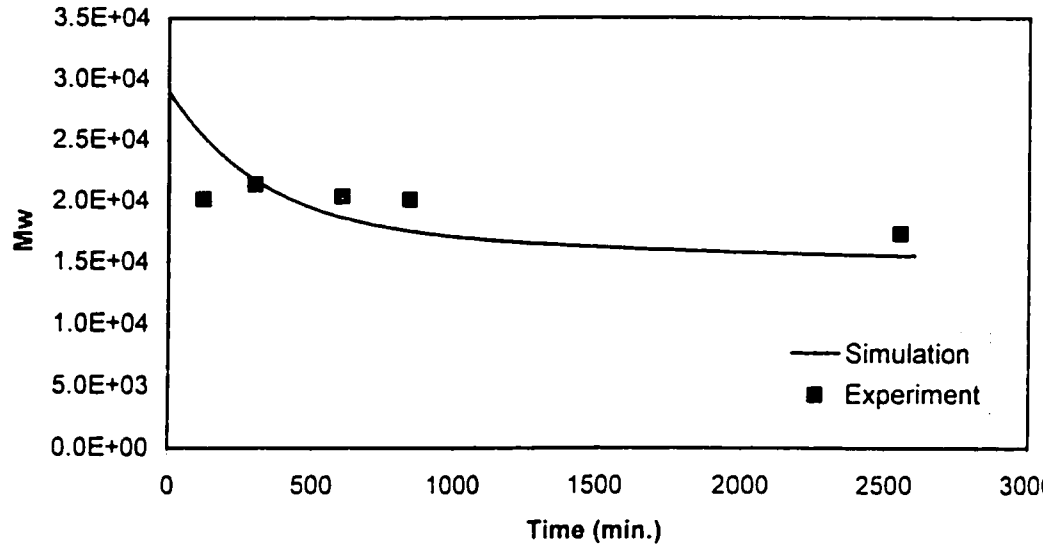

Figure 5.4.2.3 $\overline{M}_w$ vs. time for MMA/α-ms copolymerization at 115°C. MMA:α-ms = 60:40 (weight ratio), [Trigonox B] as initiator = 4.0 wt%. (Data from Palmer, 1999)

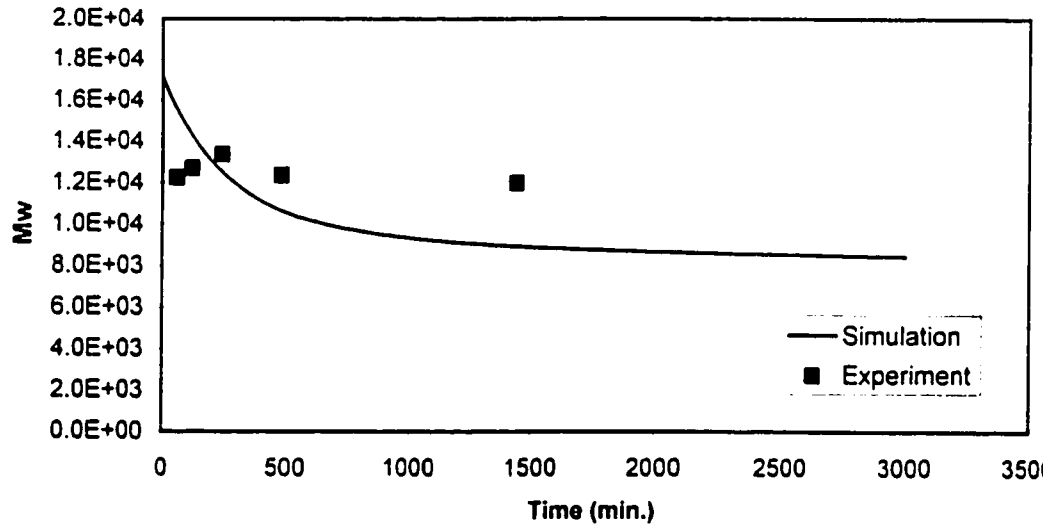

Figure 5.4.2.4 $\overline{M}_w$ vs. time for MMA/α-ms copolymerization at 115°C. MMA: α-ms = 55:45 (weight ratio), [Trigonox B] as initiator = 8.0 wt%. (Data from Palmer, 1999)

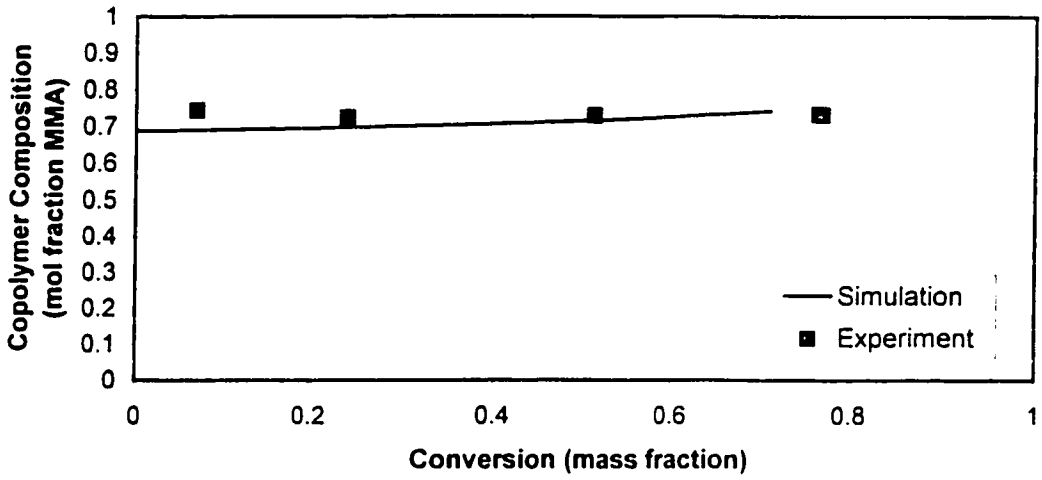

Figure 5.4.2.5 Cumulative copolymer composition vs. conversion for MMA/α-ms copolymerization at 115°C. MMA:α-ms = 60:40 (weight ratio), [Trigonox B] as initiator = 4.0 wt%. (Data from Palmer, 1999)

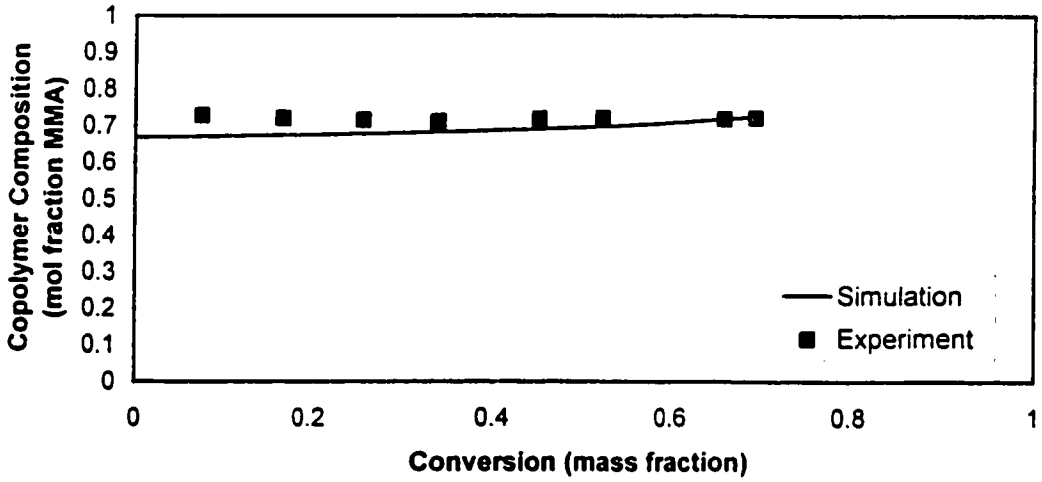

Figure 5.4.2.6 Cumulative copolymer composition vs. conversion for MMA/α-ms copolymerization at 115°C. MMA:α-ms = 55:45 (weight ratio), [Trigonox B] as initiator = 8.0 wt%. (Data from Palmer, 1999)

5.4.3 Copolymerization of MMA/α-ms at 120°C

The experimental results obtained during this study for conversion versus time at 120°C are shown along with simulation data in Figures 5.4.3.1 and 5.4.3.2 below.

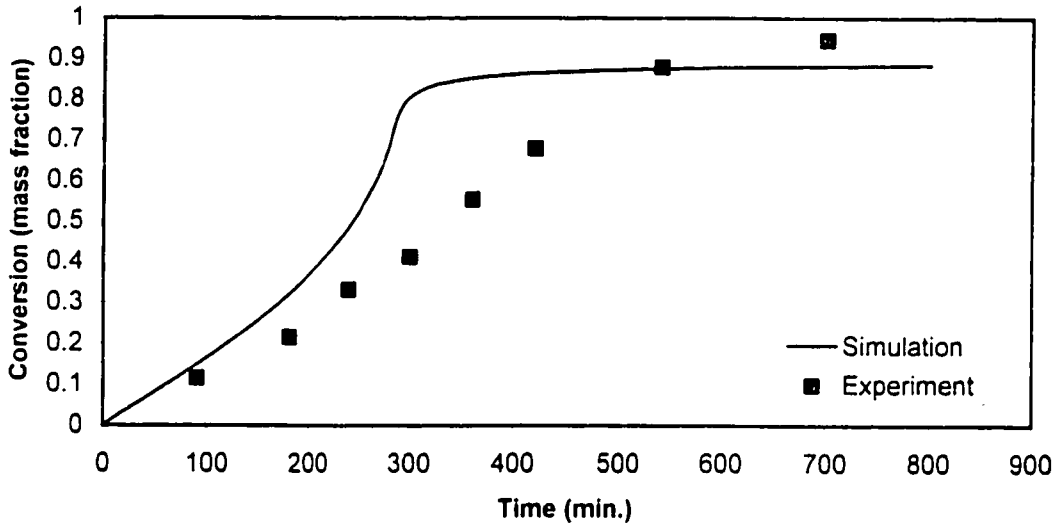

Figure 5.4.3.1 Conversion vs. time for MMA/α-ms copolymerization at 120°C. MMA: α-ms = 80:20 (weight ratio), [Trigonox B] as initiator = 0.25 wt%.

The simulation data for conversion versus time at 120°C are not as good as those made at the other temperature levels examined in this study. Poor $\overline{M}_w$ predictions, as shown in Figures 5.4.3.3 and 5.4.3.4, or poor diffusion-control parameters for α-ms are likely to blame. The problems with diffusion-control calculations are similar to the ones observed at 115°C.

When the calculation of diffusion-controlled termination effects were disabled in the program, the agreement between simulated data for conversion versus time was significantly improved at low conversion (where diffusion-controlled termination effects were at a minimum). At high conversion, diffusion-control effects were significant in the runs performed at 120°C, so it was not possible to obtain accurate high conversion predictions by disabling diffusion control-effects (as was possible at 115°C).

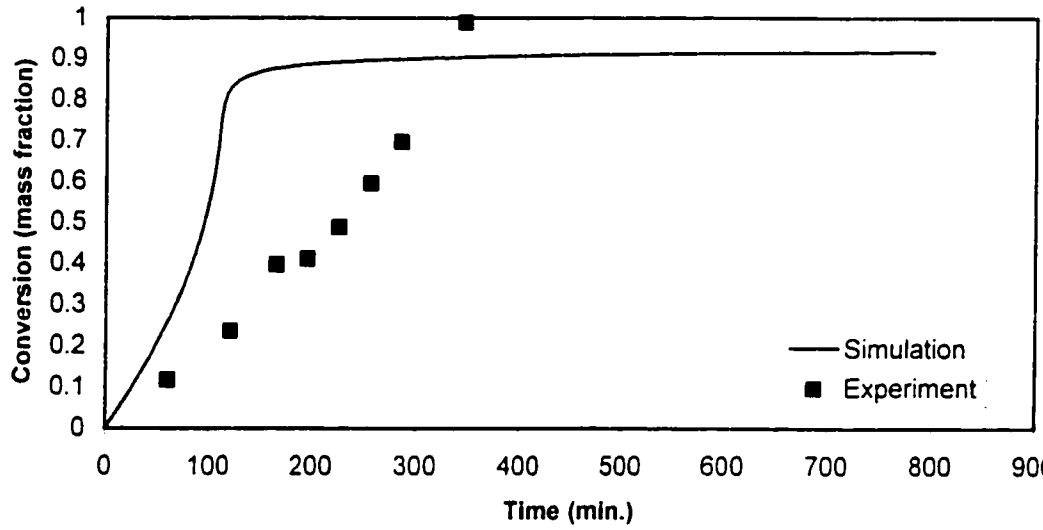

Figure 5.4.3.2 Conversion vs. time for MMA/α-ms copolymerization at 120°C. MMA: α-ms = 90:10 (weight ratio), [Trigonox B] as initiator = 0.25 wt%.

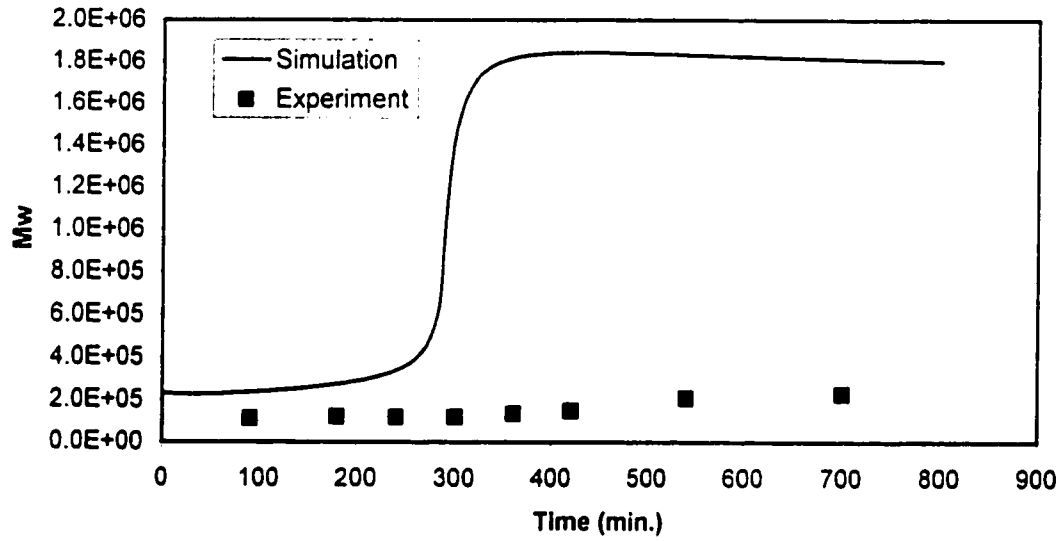

Figure 5.4.3.3 $\overline{M}_w$ versus time for MMA/α-ms copolymerization at 120°C. MMA: α-ms = 80:20 (weight ratio) , [Trigonox B] as initiator = 0.25 wt%.

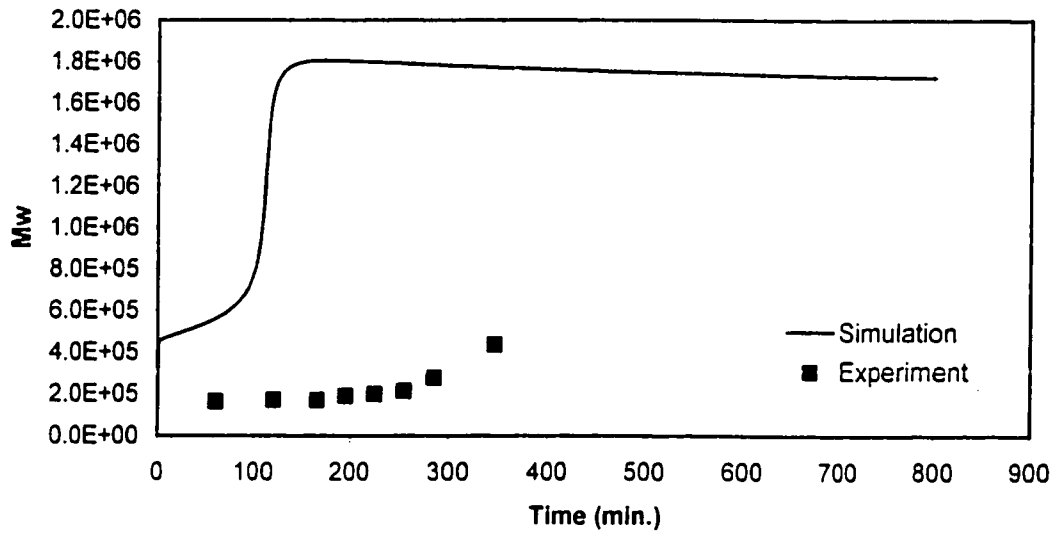

Figure 5.4.3.4 $\overline{M}_w$ versus time for MMA/α-ms copolymerization at 120°C. MMA:α-ms = 90:10 (weight ratio), [Trigonox B] as initiator = 0.25 wt%.

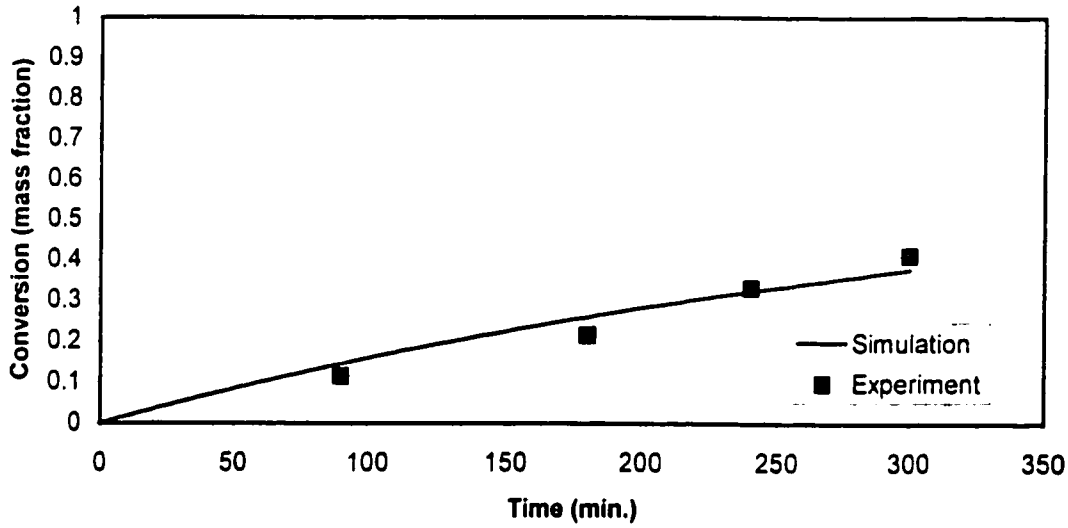

Figure 5.4.3.5 Conversion versus time for MMA/α-ms copolymerization at 120°C with diffusion-controlled termination effects disabled. MMA:α-ms = 80:20 (weight ratio), [Trigonox B] as initiator = 0.25 wt%.

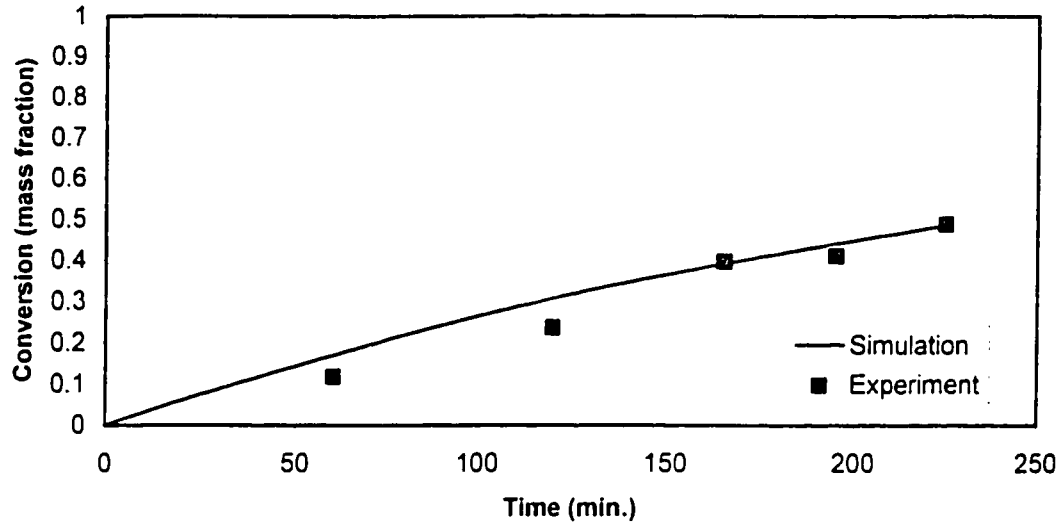

Figure 5.4.3.6 Conversion versus time for MMA/α-ms copolymerization at 120°C with diffusion-controlled termination effects disabled. MMA:α-ms = 90:10 (weight ratio) , [Trigonox B] as initiator = 0.25 wt%.

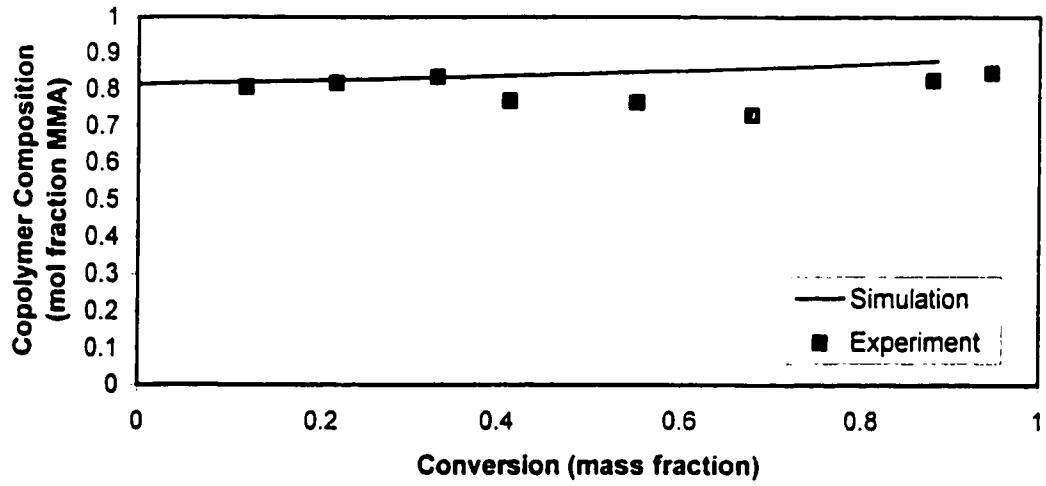

Figure 5.4.3.7 Copolymer composition versus conversion for MMA/α-ms copolymerization at 120°C. MMA:α-ms = 80:20 (weight ratio) , [Trigonox B] as initiator = 0.25wt%

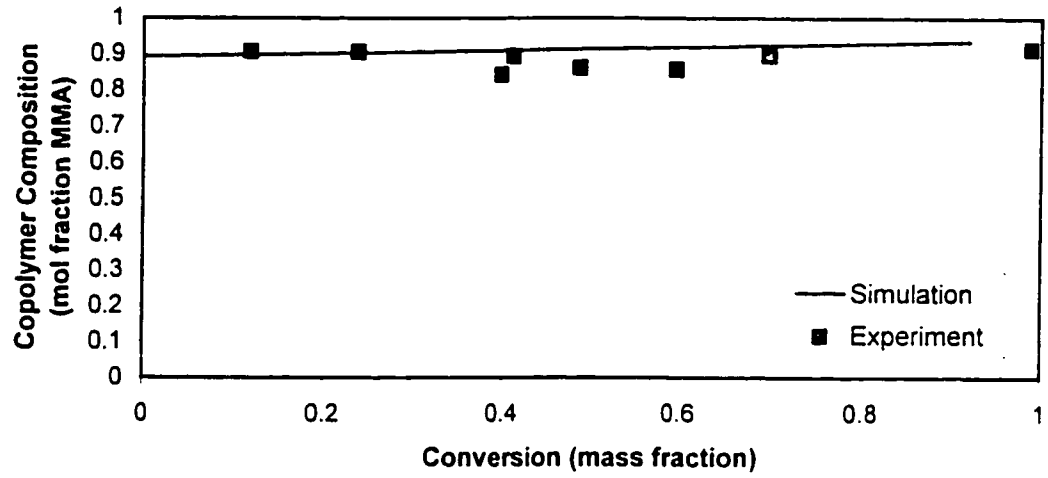

Figure 5.4.3.8 Copolymer composition versus conversion for MMA/α-ms copolymerization at 120°C. MMA:α-ms = 90:10 (weight ratio) , [Trigonox B] as initiator = 0.25 wt%.

Simulation data for copolymer composition and experimentally determined values are shown in Figures 5.4.3.7 and 5.4.3.8 above. As can be seen in the figures, the simulation data follow experimental data closely in all cases.

5.4.4 Copolymerization of MMA/α-ms at 140°C

The experimental data obtained at 140°C were taken from Palmer (1999). This data is perhaps the most interesting because depropagation effects are significant for both monomers at this temperature level. This is the first published use of a general mechanistic model to describe both the conversion profile and copolymer composition of a free-radical copolymer system where the depropagation of both monomers is significant.

The experimental data at 140°C shows similar trends as those observed at 115°C. Diffusion-controlled termination effects had to be disabled in the program in order to achieve accurate conversion versus time prediction, as was the case at 115°C.

With diffusion-controlled termination effects disabled, the simulation data for conversion versus time as shown in Figures 5.4.4.1 – 5.4.4.3 were found to follow the trends in the experimental data closely.

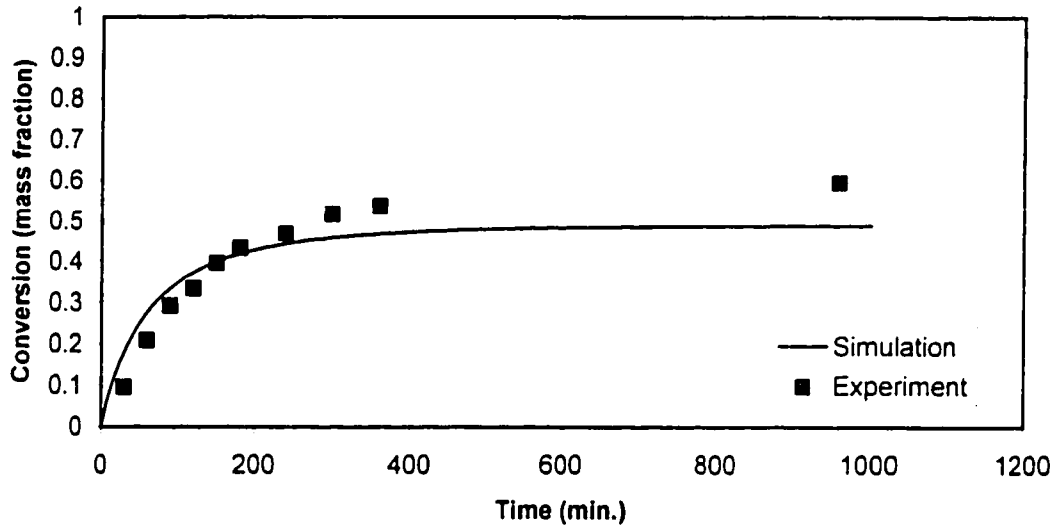

Figure 5.4.4.1 Conversion versus time for MMA/α-ms copolymerization at 140°C. MMA:α-ms = 55:45 (weight ratio) , [Trigonox B] as initiator = 0.5 wt%. (Data from Palmer, 1999)

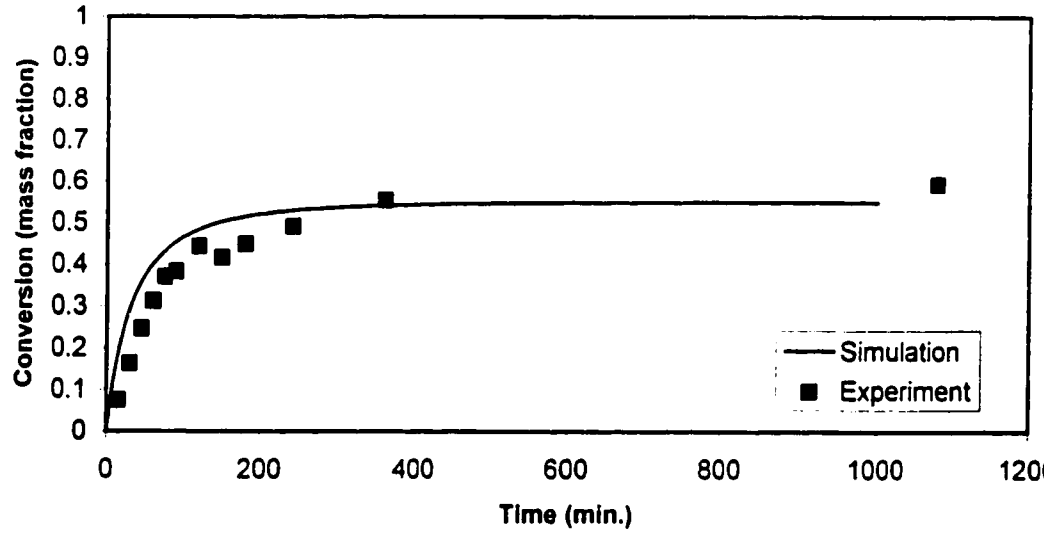

Figure 5.4.4.2 Conversion versus time for MMA/α-ms copolymerization at 140°C. MMA:α-ms = 55:45 (weight ratio) , [Trigonox B] as initiator = 2.0 wt%. (Data from Palmer, 1999)

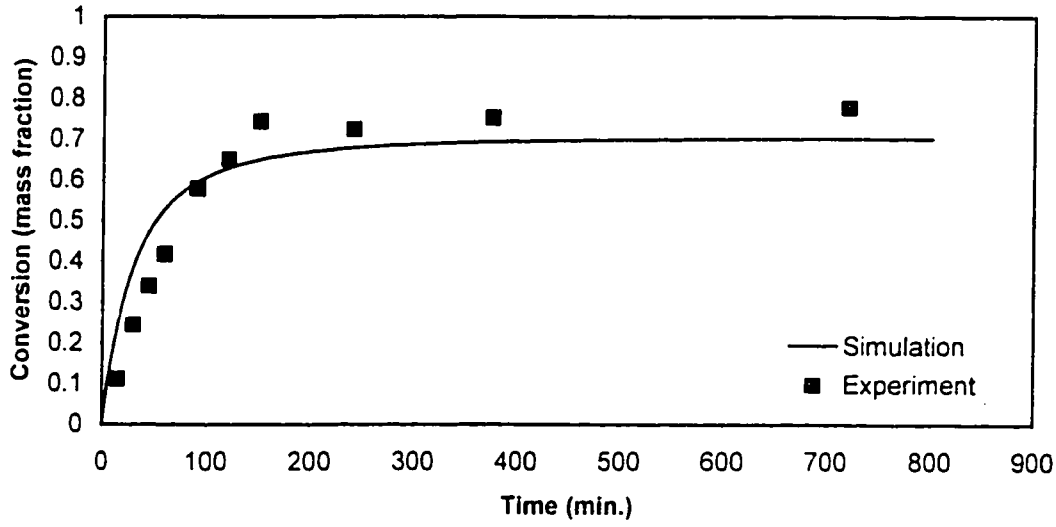

Figure 5.4.4.3 Conversion versus time for MMA/α-ms copolymerization at 140°C. MMA:α-ms = 71:29 (weight ratio) , [Trigonox B] as initiator = 1.0 wt%. (Data from Palmer, 1999)

The predictions for $\overline{M}_w$, shown in Figures 5.4.4.4 –5.4.4.6, are poor, and may again be the cause of poor diffusion-controlled termination calculations. However, since the data show no evidence of diffusion-controlled termination effects, good conversion versus time predictions were obtainable by disabling the calculation of diffusion-controlled termination effects.

Experimental and simulation data for cumulative copolymer composition versus conversion at 140°C are shown in Figures 5.4.4.7 – 5.4.4.9. As can be seen in the figures, simulation data for copolymer composition agree closely with experimental data.

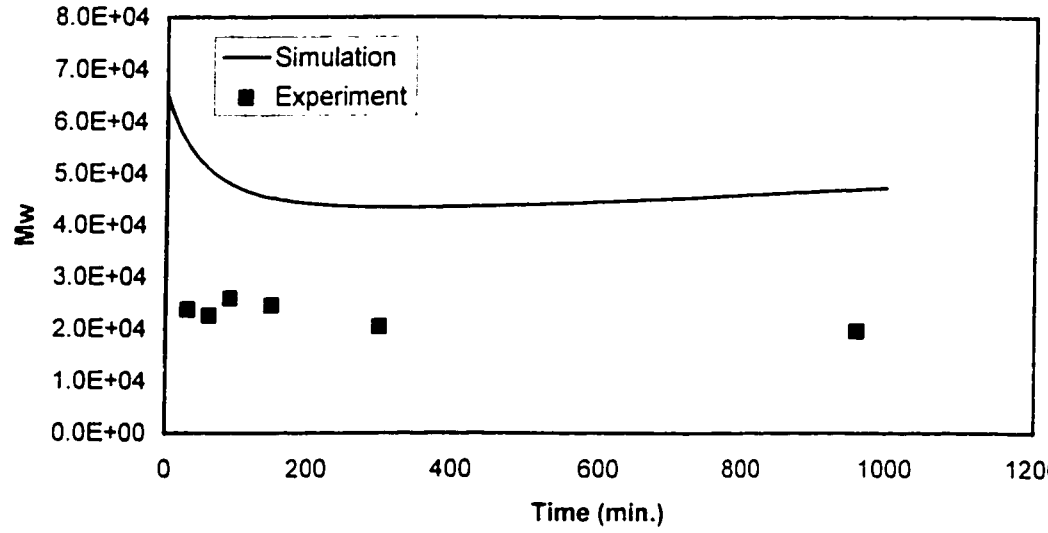

Figure 5.4.4.4 $\overline{M}_w$ versus time for MMA/α-ms copolymerization at 140°C. MMA: α-ms = 55:45 (weight ratio) , [Trigonox B] as initiator = 0.5 wt%. (Data from Palmer, 1999)

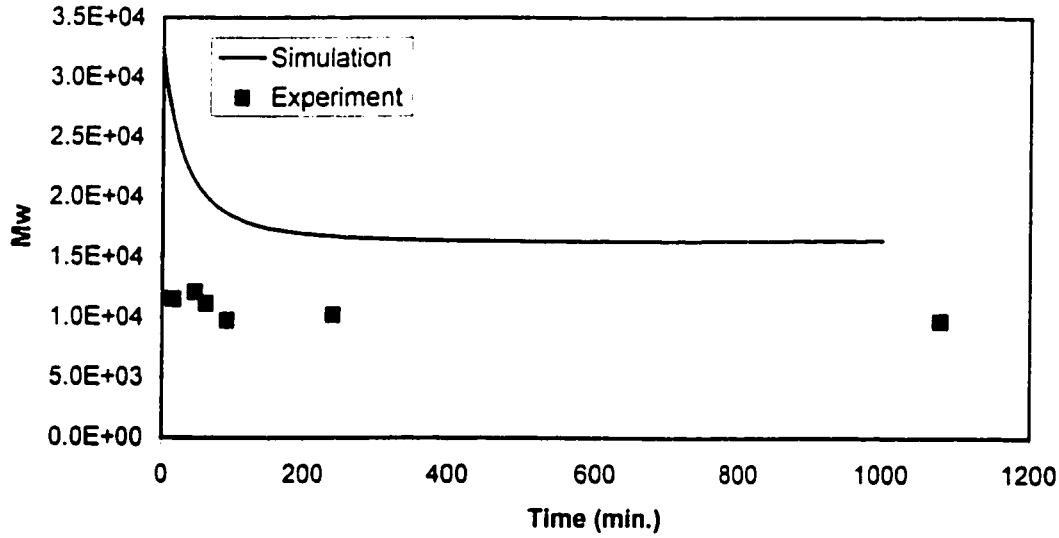

Figure 5.4.4.5 $\overline{M}_w$ versus time for MMA/α-ms copolymerization at 140°C. MMA: α-ms = 55:45 (weight ratio) , [Trigonox B] as initiator = 2.0 wt%. (Data from Palmer, 1999)

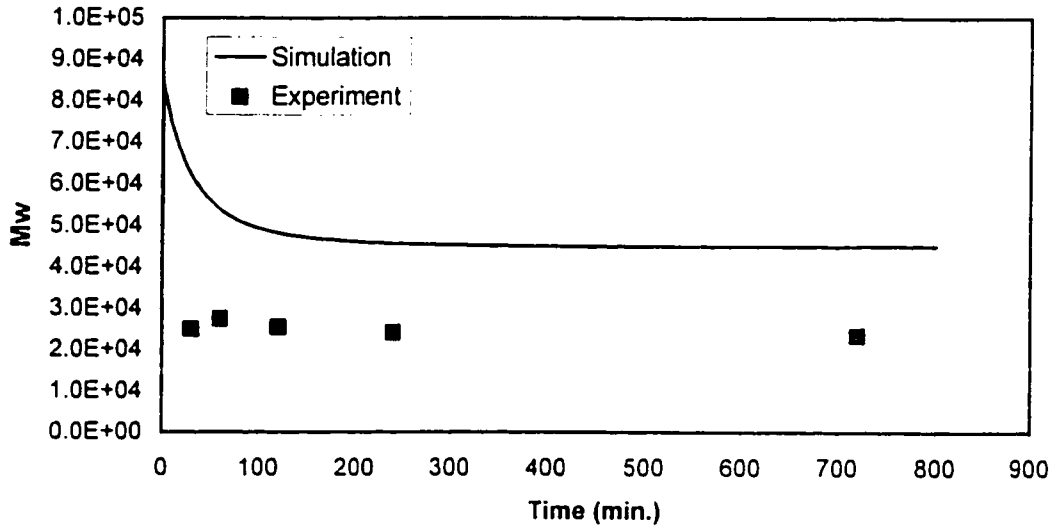

Figure 5.4.4.6 $\overline{M}_w$ versus time for MMA/α-ms copolymerization at 140°C. MMA:α-ms = 71:29 (weight ratio) , [Trigonox B] as initiator = 1.0 wt%. (Data from Palmer, 1999)

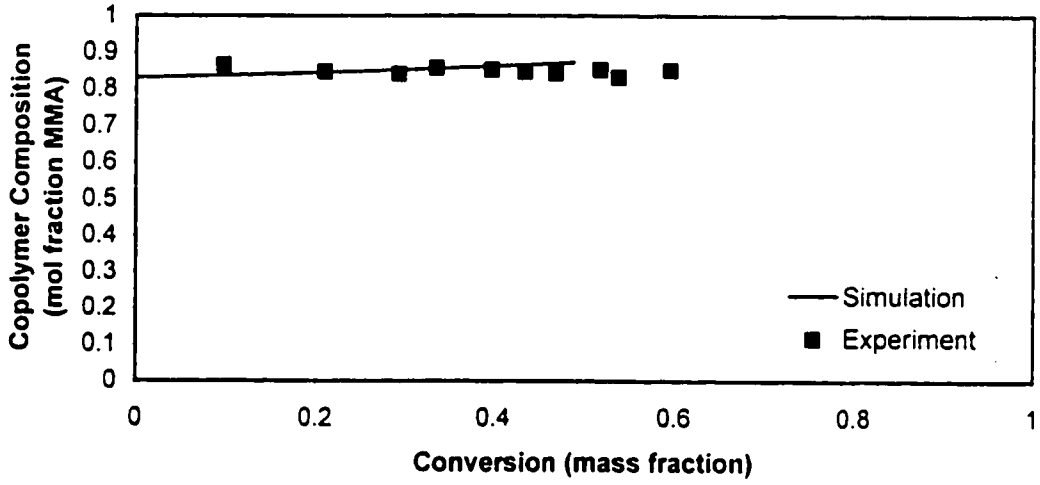

Figure 5.4.4.7 Copolymer composition versus conversion for MMA/α-ms copolymerization at 140°C. MMA:α-ms = 55:45 (weight ratio) , [Trigonox B] as initiator = 0.5wt%. (Data from Palmer, 1999)

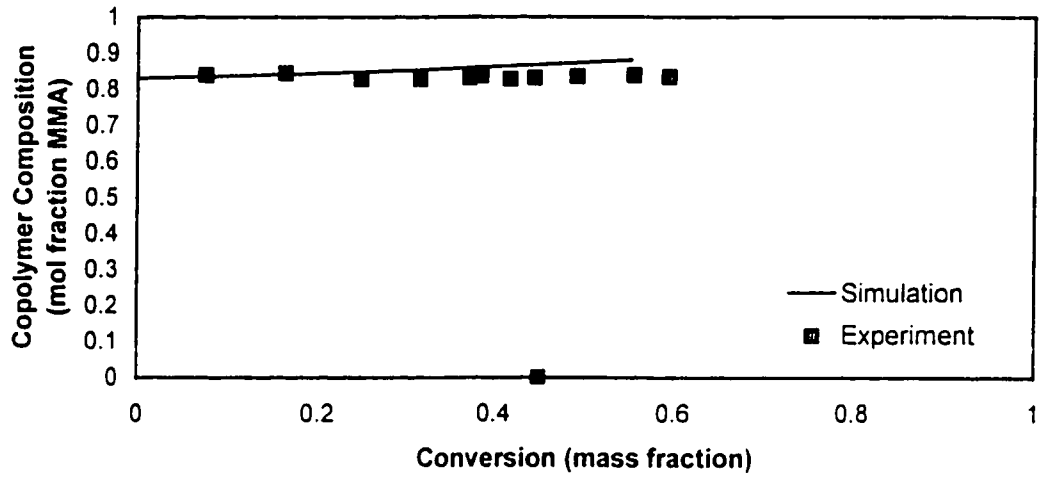

Figure 5.4.4.8 Copolymer composition versus conversion for MMA/α-ms copolymerization at 140°C. MMA:α-ms = 55:45 (weight ratio) , [Trigonox B] as initiator = 2.0 wt%. (Data from Palmer, 1999)

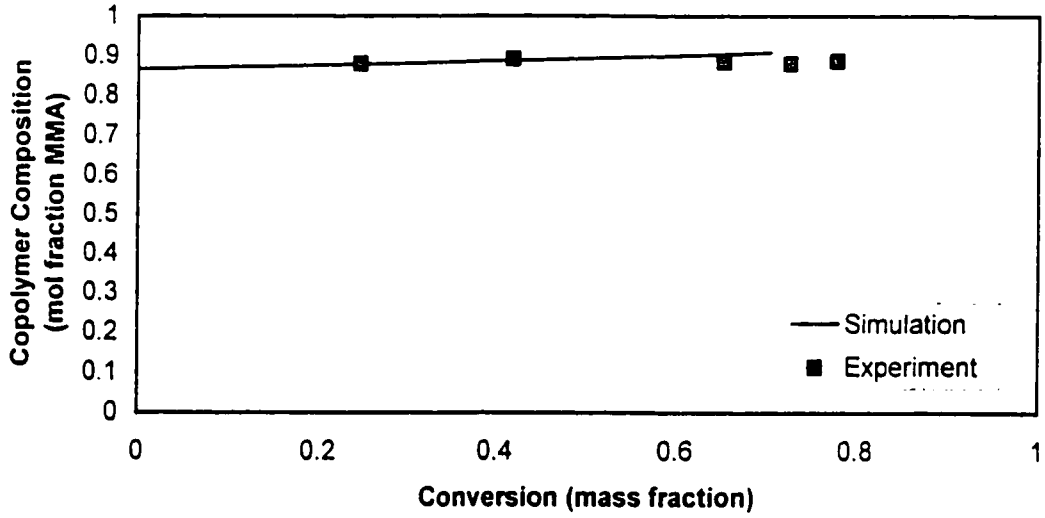

Figure 5.4.4.9 Copolymer composition versus conversion for MMA/α-ms copolymerization at 140°C. MMA:α-ms = 71:29 (weight ratio) , [Trigonox B] as initiator = 1.0 wt%. (Data from Palmer, 1999)

Overall, the program's ability to predict conversion versus time and copolymer composition is quite good when diffusion-controlled termination effects are negligible. Simulation data for the weight-average molecular weight, $\overline{M}_w$, need improvement. This may be achieved by either changes to the molecular-weight moment equations to better account for the effects of depropagation or through better values of model parameters at higher temperatures, or possibly both.

Conclusions and Recommendations

The ultimate objective of polymerization modeling efforts would be to develop a model with the ability to describe every polymerization carried out under any reaction conditions imaginable. Collectively, the objectives of this thesis were a step in the direction of reaching that lofty goal. As stated in Chapter 1, one of the objectives of this study was to implement a model in a program that could describe homopolymerization and copolymerization reactions at normal and elevated temperatures, in cases where depropagation of one or both monomers could not be ignored. The model development was explored in Chapter 2. The second objective, comparison of simulation data against experimental data, was aided by the collection of data as described in Chapter 3. The third objective of verifying the suitability of Java™ to develop a polymerization simulation was carried out by the development of the Java™ program that was described in Chapter 4. The experimental and simulation data that were presented in Chapter 5 demonstrated the program's abilities and limitations with regard to simulating polymer systems at normal and elevated temperatures.

6.1 Conclusions

The findings of this study are summarized and enumerated below.

1) The model was found to be suitable for describing the homopolymerization of the monomer methyl methacrylate at normal and elevated temperatures.

2) The model was found to adequately describe the conversion versus time profiles of methyl methacrylate/α-methylstyrene copolymers when diffusion-controlled termination effects were negligible.
3) Conversion versus time profiles could not be adequately simulated when diffusion-controlled termination effects were significant. The cause of the poor quality of the predictions may be related to inadequate diffusion-control parameters for α-methylstyrene, or due to poor weight-average molecular weight predictions.
4) Weight-average molecular weight predictions were found to be better at 100°C than at 115, 120 and 140°C. This may be due to uncertainty in model parameters at higher temperatures, or inadequacy in the modified moment equations to account for depropagation.
5) The model was found to produce excellent predictions of copolymer composition in all of the cases that were examined.
6) The Java™ programming language was found to be suitable for the development of the polymerization simulation program. Performance of the language was found to be adequate while the relatively simple language syntax and object-oriented program structure simplified the development process.

6.2 Recommendations

Based on the findings in the study, the following recommendations for future work can be made.

1) Improvements to the weight-average molecular weight predictions are required. Better predictions may be obtained by measuring parameters that affect molecular weight at high temperatures, such as chain transfer parameters. It may also be necessary to modify the existing model for

molecular weight predictions to better account for the effects of depropagation, or seek a different method entirely.

2) Although copolymer composition predictions were found to be very good, predictions were based on a parameter with a large degree of uncertainty. The parameter R_{AA} for methyl methacrylate, as described in the model of Kruger (1987), should be measured more precisely.

3) Parameters for the diffusion-controlled termination model equations are of unknown reliability for α-methylstyrene. Modification of these parameters may be necessary once correct molecular weight predictions can be made.

References

Achilias, D. and C. Kiparissides, "Modeling of Diffusion-Controlled Free-Radical Polymerization Reactors", J. Appl. Polym. Sci., **35**, 1303 (1988)

Bywater, S., "Photosensitized Polymerization of Methyl Methacrylate in Dilute Solution above 100°C", Trans. Faraday Soc., **51** 1267 (1955)

Broadhead, T. O., A. E Hamielec and J.F. MacGregor, "Dynamic Modeling of the Batch, Semi-batch and Continuous Production of styrene/butadiene Copolymers by Emulsion Polymerization", Makromol. Chem., Suppl. **10/11**, 105 (1985)

Dubé, M.A. "A Systematic Approach to the Study of Multicomponent Polymerization Kinetics", Ph.D. Thesis, University of Waterloo, Waterloo, Ontario, Canada (1994)

Dubé, M.A., J.B.P. Soares, A. Penlidis and A.E. Hamielec, "Mathematical Modelling of Multicomponent Chain-growth Polymerizations in Batch, Semi-batch and Continuous Reactors: A Review", Ind. Eng. Chem. Res., **36**, 966 (1997)

Dubé, M.A., N.M. McManus and A. Penlidis, Unpublished data. Dept. of Chemical Engineering, University of Waterloo. (1995)

Gao, J. and A. Penlidis, "A Comprehensive Simulator/Database Package for Reviewing Free-Radical Homopolymerizations", J.M.S.-Rev. Macromol. Chem. Phys. **C36** (2), 199 (1996)

Gao, J. and A. Penlidis, "A Comprehensive Simulator/Database Package for Reviewing Free-Radical Copolymerizations", J.M.S.-Rev. Macromol. Chem. Phys. **C38** (4), 651 (1998)

Gosling, J., B. Joy and G. Steele, "The Java Language Specification", Sun Microsystems (1996)

Hamielec, A.E., J.F. MacGregor and A. Penlidis "Copolymerization", in "Comprehensive Polymer Science", Sir G. Allen, Ed., Pergamon Press, Oxford, U.K., **3**, 17 (1989)

Howell, J.A., Masatsugu Izu and K.F. O'Driscoll, "Copolymerization with Depropagation. III. Composition and Sequence Distribution from Probability Considerations", J. Polym. Sci. Part A-1, **8**(3), 699-710 (1970)

Ito, K. and K. Kodaira, "Kinetics of Radical Copolymerization between α-Methylstyrene and Methyl Methacrylate", Polymer Journal, **18**(9), 667-672 (1986)

Ivin, K.J. and R.H. Spensley, "Copolymerization Systems Involving Reversible Propagation Steps", J. Macromol. Sci. Chem., **A1**(4), 653 (1967)

Izu, M. and K.F. O'Driscoll, "Copolymerization with Depropagation. V. Copolymerization of α-Methylstyrene and Methyl Methacrylate between Their Ceiling Temperatures", **8**(7) (1970)

Izu, M., K.F. O'Driscoll, R.J. Hill, M. J. Quinn, and H. J. Harwood. "Coisotacticities in the Free-Radical Copolymerization of α-Methylstyrene and Methyl Methacrylate between Their Ceiling Temperatures", **5** (1972)

Jaworski, J., "Java 1.1 Developer's Guide", Second Edition., Sams.net, Indiana (1997)

Kang, B.K. and K.F. O'Driscoll, "Copolymerization with Depropagation. IX. Molecular Weights in Copolymerization with Depropagation", Macromolecules, **42** (1960)

Kukulj, D. and T.P. Davis, "Average Propagation Rate Coefficients in the Free-Radical Copolymerization of Styrene and α-Methylstyrene Measured by Pulsed-Laser Polymerization", Macromolecules, **31**, 5668-5680 (1998)

Kuindersma, M.E., "On the Modelling of Free-Radical Polymerization Reactions: Homopolymerization", M.A.Sc. thesis, Department of Chemical Engineering, University of Waterloo (1992)

Mahabadi, H.K. and K.F. O'Driscoll. "Absolute Rate Constants in Free-Radical Polymerization. III. Determination of Propagation and Termination Rate Constants for Styrene and Methyl Methacrylate", J. Macromol. Sci.-Chem., **A11**, 967 (1977).

Marten, F.L. and A.E. Hamielec, "High-Conversion Diffusion-Controlled Polymerization", in ACS Symposium Series, H.N. Henderson and T.C. Bouton, Eds., American Chemical Society, Washington, DC, **104**, 43 (1979)

Martinet, F. and J. Guillot, "Copolymerization with Depropagation: Experiments and Prediction of Kinetics and Properties of α-Methylstyrene - Methyl Methacrylate Copolymers. I. Solution Copolymerization", J. App. Polym. Sci. **65** (12), 2297 (1996)

Martinet, F. and J. Guillot, "Copolymerization with Depropagation: Prediction of Kinetics and Properties of α-Methylstyrene - Methyl Methacrylate Copolymers. II. Bulk Copolymerization", J. App. Polym. Sci. **72** (12), 1611-1625 (1999a)

Martinet, F. and J. Guillot, "Copolymerization of α-Methylstyrene with Methyl Methacrylate. III. Emulsion Process: Experimental Data on Kinetics, Particle Size, Composition, Molecular Weight, and Glass Transition Temperature", J. App. Polym. Sci. **72** (12), 1627-1645 (1999b)

Odian, G., "Principles of Polymerization", Third Edition. Wiley-Interscience, New York (1991)

O'Driscoll, K.F. and F.P. Gasparro, "Copolymerization with Depropagation", J. Macromol. Sci. Chem., **A1**(4), 643 (1967)

Otsu, T, B. Yamada, T. Mari and M. Inoue, J. Polym. Sci., Polym. Lett. Ed., **14**, 283 (1976)

Palmer, D.E., "The Copolymerization of Methyl Methacrylate and α-Methyl Styrene in Bulk and Solution at Elevated Temperatures", M.A.Sc. thesis, University of Waterloo, Waterloo, Ontario, Canada (1999)

Polymer Handbook, J. Brandrup and E.H. Immergut (Eds.), Wiley, New York. (1989)

Press,W. and W. Vetterling, "Numerical Recipes in C: the Art of Scientific Computing", 2nd edition, Cambridge University Press (1994)

Ray, W.H., "Practical Benefits from Modeling Olefin Polymerization Reactors", in Transition Metal Catalyzed Polymerization, Quirk, R.P., Ed.; Harwood: New York (1988)

Russell, G. T., R.G. Gilbert, D.H. Napper, "Termination in Free-Radical Polymerizing Systems at High Conversion.", Macromolecules, **21**, 2133 (1988)

Stickler, M., D. Panke and A.E.Hamielec, "Polymerization of Methylmethacrylate up to High Degrees of Conversion: Experimental Investigation of the Diffusion-Controlled Polymerization." J. Polym. Sci., Polym. Chem. Ed., **22**, 2243 (1984)

Stickler, M., "Experimental Techniques in Free Radical Polymerization Kinetics", Makromol. Chem., Macromol. Symp., **10/11**, 17-70 (1987)

Weickert, G., "Hollow Shaft Reactor: a Useful Tool for Bulk Polymerizations at High Viscosities, Temperatures, and Polymerization Rates", Ind. Eng. Chem. Res. **37**, 799 (1998)

Wittmer, P., "Copolymerization in the Presence of Depolymerization Reactions", Adv. Chem. Ser., **99**, 140 (1971)

Xie, T. and A.E. Hamielec, "Modeling Free-Radical Copolymerization Kinetics – Evaluation of the Pseudo-Kinetic Rate Constant Method, 1. Molecular Weight Calculation for Linear Copolymers." Makromol. Chem., Theory Simul. **2**, 421 (1993a)

Xie, T. and A.E. Hamielec, "Modeling Free-Radical Copolymerization Kinetics – Rvaluation of the Pseudo-Kinetic Rate Constant Method, 1. Molecular Weight Calculations for Copolymers with Long Chain Branching." Makromol. Chem., Theory Simul. **2**, 455 (1993b)

Zhuang, J., S. Das, M.D. Nowakowski and S.C. Greer, "Living poly(α-methylstyrene) near the polymerization line 6. Chemical kinetics", Physica A, **244**, 522 (1997)

Appendix A

Copolymerization with Depropagation Model Development and Solution Methodology

DISCLAIMER: The following derivation is taken directly from Kruger et al. (1987) and is included here for two reasons. Firstly, the original paper is written in German and a translation is not easily obtainable. Secondly, these equations are rather complex and it is important for future model development that they be made available here.

Kruger's nomenclature is different than the nomenclature used in the main body of this thesis. He uses A and B to denote the different monomer species (M_1 and M_2 were used in the nomenclature of this thesis). Species that bear a free radical are denoted with a "+". The propagation rate constants are denoted simply as k (rather than k_p in the previous nomenclature) while the reverse polymerization rate constant is denoted as k^- (rather than k_{dp}).

A.1 Derivation of the Model

For the kinetics of reversible copolymerisation, the four possible reactions are assumed to be independent of the polymer structure and include:

$$\sim\sim A^* + A \underset{k^-_{AA}}{\overset{k_{AA}}{\rightleftharpoons}} \sim\sim AA^* \tag{2}$$

$$\sim\sim A^* + B \underset{k^-_{AB}}{\overset{k_{AB}}{\rightleftharpoons}} \sim\sim AB^* \tag{3}$$

$$\sim\sim B^* + A \underset{k^-_{BA}}{\overset{k_{BA}}{\rightleftharpoons}} \sim\sim BA^* \tag{4}$$

$$\sim\sim B^* + B \underset{k^-_{BB}}{\overset{k_{BB}}{\rightleftharpoons}} \sim\sim BB^* \tag{5}$$

The change in concentration of the different species with respect to time is described by the following differential equations:

$$-\frac{d[A]}{dt} = k_{AA}[A][A^*] - k^-_{AA}[AA^*] + k_{BA}[A][B^*] - k^-_{BA}[BA^*] \tag{6}$$

$$-\frac{d[B]}{dt} = k_{AB}[B][A^*] - k_{AB}^-[AB^*] + k_{BB}[B][B^*] - k_{BB}^-[BB^*] \tag{7}$$

$$-\frac{d[A^*]}{dt} = \frac{d[B^*]}{dt} = k_{AB}[B][A^*] - k_{AB}^-[AB^*] - k_{BA}[A][B^*] + k_{BA}^-[BA^*] \tag{8}$$

The change in concentration with respect to time of the endgroup pairs ~~~XY*, is shown below for like-monomer pairs here:

$$-\frac{d[AA^*]}{dt} = -k_{AA}[A][BA^*] + k_{AA}^-[BAA^*] + k_{AB}[B][AA^*] - k_{AB}^-[AAB^*] \tag{9}$$

$$-\frac{d[BB^*]}{dt} = -k_{BB}[B][AB^*] + k_{BB}^-[ABB^*] + k_{BA}[A][BB^*] - k_{BA}^-[BBA^*] \tag{10}$$

By the introduction of conditional probabilities of the monomer pair or triad concentrations on the appropriate radical concentration [A^*] or [B^*], the following relations are obtained:

$$[BA^*] + [AA^*] = [A^*] \qquad \begin{aligned} [AA^*] &= P_{AA}[A^*] \\ [BA^*] &= P_{AB}[A^*] \end{aligned} \tag{11}$$

$$[BAA^*] + [AAA^*] = [AA^*] \qquad \begin{aligned} [AAA^*] &= P_{AA}^2[A^*] \\ [BAA^*] &= P_{AA}P_{AB}[A^*] \end{aligned} \tag{12}$$

The conditional probability P_{XY} is understood to mean an active center X^* is attached to the polymer chain by a y-unit.

For the further derivation of the model, the following two statements are assumed:

1. The stationary-state hypothesis applies to each type of active center (A^*, AA^*, AAA^*).

2. The developing macromolecules are sufficiently large so that effects of the chain ends may be neglected and thus, the monomer pair distributions of the copolymers can be calculated from the conditioned probabilities P_{XY}.

By the ratio d[A]/d[B] from equations (6) and (7) and by combination with equations (11) and (12),

$$f = \frac{d[A]}{d[B]} = \frac{[A^*](k_{AA}[A] - k_{AA}^- P_{AA} - k_{BA}^- P_{AB}) + [B^*]k_{BA}[A]}{[B^*](k_{BB}[B] - k_{BB}^- P_{BB} - k_{AB}^- P_{BA}) + [A^*]k_{AB}[A]} \tag{13}$$

is obtained. Applying the stationary-state hypothesis -d[A+]/dt = 0 to equation 8 and solving for [A^*], the following equation is obtained:

$$[A^*] = [B^*]\frac{k_{BA}[A] + k_{AB}^- P_{BA}}{k_{AAB}[B] + k_{BA}^- P_{AB}} \tag{14}$$

By using equation (14) and introducing the reactivity ratios:

$$r_A = \frac{k_{AA}}{k_{AB}}, \quad r_B = \frac{k_{BB}}{k_{BA}}, \quad r_A = \frac{k_{AA}}{k_{AB}}, \quad R_A = \frac{k_{AB}^-}{k_{BA}},$$
$$R_B = \frac{k_{BA}^-}{k_{AB}}, \quad R_{AA} = \frac{k_{AA}^-}{k_{AB}}, \quad R_{BB} = \frac{k_{BB}^-}{k_{BA}} \tag{15}$$

the following relation is obtained by substitution into equation (13):

$$f = \frac{[A]\{r_A([A] + R_A P_{BA}) + [B] - R_{AA} P_{AA}\} - R_A P_{BA}(R_{AA} P_{AA} + R_B P_{AB})}{[B]\{r_B([B] + R_B P_{AB}) + [A] - R_{BB} P_{BB}\} - R_B P_{AB}(R_{BB} P_{BB} + R_A P_{BA})} \tag{16}$$

Equation (16) establishes an analytical relation between a given monomer mixture and the copolymer formed during the initial stages of a copolymerization reaction. The constant r_A (r_B) represents the measure of uptake of monomer A (B) or B (A) by an active center A^* (B^*) (analogous to irreversible copolymerization). The parameters R_A (R_B) describe the ratio of new entities of active centers A^* (B^*) by separation of B (A) or combination of A (B) with the active center B^* (A^*). R_{AA} (R_{BB}) is the ratio of the constant of the extermination of active centers AA^* (BB^*) by separation of A (B) or combination with B (A).

The conditional equations for equation (16) and their partly occurring probabilities P_{AB} and P_{BA} can be deduced from the stationary conditions $d[AA^*]/dt = 0$ and $d[BB^*]/dt = 0$ (equation (9) and (10) as well as equation (14)):

$$0 = -k_{AA}^{-} P_{AA} P_{AB} [A^*] + k_{AA} P_{AB} [A][A^*] - k_{AB} P_{AA} [B][A^*] + k_{AB}^{-} P_{AA} P_{BA} \frac{k_{AB}[B] + k_{BA}^{-} P_{AB}}{k_{BA}[A] + k_{AB}^{-} P_{BA}} [A^*] \tag{17}$$

$$0 = -k_{BB}^{-} P_{BB} P_{BA} [B^*] + k_{BB} P_{BA} [B][B^*] - k_{BA} P_{BB} [A][B^*] + k_{BA}^{-} P_{AB} P_{BB} \frac{k_{BA}[A] + k_{AB}^{-} P_{BA}}{k_{AB}[B] + k_{BA}^{-} P_{AB}} [B^*] \tag{18}$$

By introducing the parameters r_i, R_i and R_{ii}, elimination of $[A^*]$ and $[B^*]$ and applying the relations $P_{AB} + P_{AA} = 1$ and $P_{BA} + P_{BB} = 1$, equations (17) and (18) become:

$$bP_{AB}^2 + (r_A[A] + [B]a - b)P_{AB} - [B]a = 0 \tag{19}$$

$$dP_{BA}^2 + (r_B[B] + [A]c - d)P_{BA} - [A]c = 0 \tag{20}$$

where

$$a = 1 - \frac{R_A P_{BA}}{[A] + R_A P_{BA}}, \quad b = R_{AA} - \frac{R_A R_B P_{BA}}{[A] + R_A P_{BA}}$$

$$c = 1 - \frac{R_B P_{AB}}{[B] + R_B P_{AB}}, \quad d = R_{BB} - \frac{R_A R_B P_{AB}}{[B] + R_B P_{AB}} \tag{21}$$

For the general cases b ≠ 0, d ≠ 0 the quadratic solution can be obtained:

$$P_{AB} = \frac{1}{2}\left[1 - \frac{r_A[A] + [B]a}{b} \pm \sqrt{\left(1 - \frac{r_A[A] + [B]a}{b}\right)^2 + \frac{4[B]a}{b}}\right] \tag{22}$$

$$P_{BA} = \frac{1}{2}\left[1 - \frac{r_B[B] + [A]c}{d} \pm \sqrt{\left(1 - \frac{r_B[B] + [A]c}{d}\right)^2 + \frac{4[A]c}{d}}\right] \tag{23}$$

The implied system of equations $P_{AB} = P_{AB}(P_{BA})$ and $P_{BA} = P_{BA}(P_{AB})$[1] can be solved in a simple iterative way, where the prevailing solutions can be chosen by $0 \leq P \leq 1$. Each of the cases $b = 0$, and $d = 0$, have to be treated separately because the quadratic equations (19) and (20) results in linear equations with the solutions:

$$P_{AB} = \frac{[B]a}{r_A[A] + [B]a}, \quad P_{BA} = \frac{[A]c}{r_B[B] + [A]c} \tag{24}$$

The following cases can be distinguished for the completion of the conditions $b = 0$, and $d = 0$:

1. $R_{AA} = R_A = R_B = R_{BB} = 0$ for b = d = 0

[1] "$P_{AB} = P_{AB}(P_{BA})$ and $P_{BA} = P_{BA}(P_{AB})$" should be read as "P_{AB} is a function of P_{BA} and P_{BA} is a function of P_{AB}".

Hence, the special case of the irreversible copolymerization with $a = c = t$ follows, i. e. the classic Mayo-equations for equation (24) result in:

$$P_{AB} = \frac{[B]}{r_A[A]+[B]}, \quad P_{BA} = \frac{[A]}{r_B[B]+[A]} \tag{25}$$

2. $R_{AA} = 0$ and $R_A = 0$ or $R_B = 0$ for $b = 0$, respectively.
   $R_{BB} = 0$ and $R_A = 0$ or $R_B = 0$ for d = 0

In this case the homo-growth rate reactions of one (or both) monomers are irreversible and one of the homo-growth rate reactions is reversible.

3. $R_{AA} \neq 0$, $R_A \neq 0$, $R_B \neq 0$, and $R_{AA} = \dfrac{R_A R_B P_{BA}}{[A]+R_A P_{BA}}$ for $b = 0$, respectively

   $R_{BB} \neq 0$, $R_A \neq 0$, $R_B \neq 0$, and $R_{BB} = \dfrac{R_A R_B P_{AB}}{[B]+R_B P_{AB}}$ for $d = 0$

Considering these conditions, the following relations between monomer concentration, reactivity ratios and partly occurring probabilities are obtained:

$$[A] = \frac{(R_B - R_{AA})R_A}{R_{AA}} P_{BA} \text{ for } b = 0$$

$$[B] = \frac{(R_A - R_{BB})R_B}{R_{BB}} P_{AB} \text{ for } d = 0 \tag{26}$$

In the cases where $b = 0$ and $d = 0$ the quotient will be:

$$\frac{[A]}{[B]} = \frac{R_{BB} R_A (R_B - R_{AA})}{R_{AA} R_B (R_A - R_{BB})} \cdot \frac{x_A}{x_B} = constant \cdot \frac{x_A}{x_B} \tag{27}$$

a correlation between monomer ratios in the monomer mixture and in the copolymer. When the rate constants are such that the resulting *constant* has a value of 1, a point of balance (azeotrope) is achieved.

A second function P_{BA} / P_{AB} results from the definition of partly occurring probabilities in an independent function of f of equation (16). However, both functions are identical for the pairs P_{AB} / P_{BA} which are solutions of the system of equations (19) and (20). The proof of the identity can be shown in a simple way by putting in the $P_{AB}(P_{BA})$ relations (22) and (23) in the corresponding f-functions.

A.2 Solving Kruger's equations

As stated above, an iterative procedure is required to obtain the partial probabilities P_{AB} and P_{BA} in the most general case of both monomers undergoing depropagation. A very simple iterative procedure that can be used to solve for these probabilities is given below:

1) Make an initial guess for P_{AB} and P_{BA}, say $P_{AB} = P_{BA} = 0.5$.
2) Calculate a and b from equation (21).
3) Calculate P_{AB} from equation (22).
4) Calculate P_{BA} from equation (23), utilizing the value of P_{AB} obtained in the previous step.
5) Repeat steps 1-4 until desired convergence is obtained.

For the MMA-AMS system, convergence from the initial guess to an accuracy of 1×10^{-9} was obtained within just 4-6 iterations.

As stated above, equation (16) establishes an analytical relation between a given monomer mixture and the copolymer formed during the initial stages of a copolymerization reaction. The equation is valid not only during the initial stages of a copolymerization reaction, but also throughout the full conversion range so long as the monomer concentrations during the copolymerization reaction are used in the equation. The monomer concentrations can be obtained at any point during a copolymerization reaction by integrating the expressions for the rates of change of monomer concentrations, equations (6) and (7). Note that these equations require the calculation of the concentrations of individual radical species, something that Kruger did not explicitly state how to do in his paper. A procedure for solving Kruger's equations for full conversion simulations is presented below.

A.3 Procedure for Solving Kruger's Equations for Full Conversion Simulations

Obtain the temperature dependent parameters in equation (15) from experiment or literature. Palmer (1999) gives values for the MMA-AMS system. Solve for the partial probabilities P_{AB} and P_{BA} according to the procedure outline above. Calculate the remaining probabilities:

$$P_{AA} = 1 - P_{AB} \tag{a3.1}$$

$$P_{AA} = 1 - P_{AB} \tag{a3.2}$$

Substitute the parameters, probabilities, and monomer concentrations into equation (16) to obtain $f = \mathrm{d}[A]/\mathrm{d}[B]$.

Calculate the overall radical concentration as given by equation 2.9.4:

$$Y_o = \frac{\left(\sum_{i=1}^{N_t} k_{ti}^2 [MSI]_i^2 + 4k_t R_i\right)^{\frac{1}{2}} - \sum_{i=1}^{N_t} k_{ti}[MSI]_i}{k_t} \tag{2.9.4}$$

Since we are dealing with a copolymer system, then it follows that:

$$Y_o = [A^*] + [B^*] \tag{a3.3}$$

Combining equations (28) and (14), and solving for $[B^*]$:

$$[B^*] = \frac{Y_o}{1 + \frac{k_{BA}[A] + k_{AB}^- P_{BA}}{k_{AAB}[B] + k_{BA}^- P_{AB}}} \tag{a3.4}$$

Calculate $[B^*]$ from equation (31), and rearrange equation (30) to solve $[A^*]$. Solve for $[AA^*]$ and $[BA^*]$ by using equation (11). Substitute the results into equation (6) to solve for -d[*A*]/d*t*. The value of -d[*B*]/d*t* is easily calculated as -d[*B*]/d*t* = (-d[*A*]/d*t*)/*f*. To obtain the solution for the model over the full conversion range, numerically integrate the differential equations using a suitable ordinary differential equation solver.

Appendix B

Experimental Data

Full Conversion Study Results

Table B1

MMA-AMS 80:20 weight ratio, 2 wt% Trig B, 100°C

Time (min.)	Conversion (mass fraction)	Mn (g/mol)	Mw (g/mol)	F AMS mol%	F MMA mol%
60	0.032	48787	70099	26.01	73.99
240	0.121	57620	79208	20.80	79.20
360	0.184	57415	81000	21.02	78.98
540	0.282	51052	77624	21.23	78.77
690	0.375	63346	90638	27.60	72.40
780	0.46	63839	91668	33.39	66.61
1020	0.571	75919	111666	21.04	78.96
1140	0.801	105323	261294	21.64	78.36
1335	1	122611	379535	18.64	81.36

Table B2

MMA-AMS 90:10 weight ratio, 2 wt% Trig B, 100°C

Time (min.)	Conversion	Mn	Mw	F AMS mol%	F MMA mol%
60	0.039	80381	116606	12.70	87.30
180	0.137	89431	132065	13.93	86.07
270	0.207	90938	133574	14.43	85.57
360	0.324	93678	139096	11.97	88.03
510	0.432	98528	155486	14.18	85.82
600	0.592	121139	236334	11.85	88.15
750	0.998			11.52	88.48
840	1			12.64	87.36

Full Conversion Study Results

Table B3

MMA-AMS 80:20 weight ratio, 0.25 wt% Trig B, 120°C

Time (min.)	Conversion (mass fraction)	Mn (g/mol)	Mw (g/mol)	F AMS mol%	F MMA mol%
90	0.115	76984	113205	19.35	80.65
180	0.215	83304	121722	18.21	81.79
240	0.331	77815	119117	16.60	83.40
300	0.412	74083	121186	23.16	76.84
360	0.552	89782	135331	23.56	76.44
420	0.677	93349	149406	27.01	72.99
540	0.879	111439	209244	17.57	82.43
700	0.946	95252	229596	15.40	84.60

Table B4

MMA-AMS 90:10 weight ratio, 0.25 wt% Trig B, 120°C

Time (min.)	Conversion	Mn	Mw	F AMS mol%	F MMA mol%
60	0.118	99596	162910	9.25	90.75
120	0.237	105096	171515	9.47	90.53
165	0.397	104318	169950	15.75	84.25
195	0.411	119724	190641	10.60	89.40
225	0.488	120121	198894	13.93	86.07
255	0.595	122802	213032	14.30	85.70
285	0.697	138244	277319	10.41	89.59
345	0.988	179783	435991	8.55	91.45
420	1.02			9.86	90.14
1620	0.965	187066	467715	8.84	91.16

Appendix C

Platform Availability of Java™ Environments

Table C1
Java Platform Ports as of Sept 24, 1999-09-29

OS	CPU	Company/Organization	Ported Technology
AIX		IBM	JDK
DG/UX 4.2	Intel	Data General Corporation	JDK
DYNIX/ptx 4.4.2 forward	Intel	Sequent Computer Systems	JDK
HP-UX		Hewlett-Packard	JDK
IRIX		Silicon Graphics	JDK
Linux		Blackdown.org	JDK
MacOS		Apple	JDK, JRE
NetWare		Novell	JNDI, NSI, JIT and Java Virtual Machine
OpenVMS	Alpha	Compaq Computer Corporation	JDK
OS/2	i386	IBM	JDK
OS/390, OS/400		IBM	JDK
SCO	i386	SCO	JDK
Tru64 UNIX	Alpha	Compaq Computer Corporation	JDK
UnixWare	i386	SCO	JDK
VxWorks		Wind River Systems	Java Virtual Machine
Windows NT	Alpha	Digital Equipment Corportation	JRE

JDK = Java Developers Kit
JRE = Java Runtime Environment
The standard JDK releases are for Windows 95/98 and Solaris, and these version are not considered to be "ports".
This information was available at http://www.javasoft.com/cgi-bin/java-ports.cgi

Appendix D

Simplified Model Derivation, Solution and Comparison with Program Output

A simplified version of the model described in this document can be solved analytically. A description of the simplified model, as well as the derivation of the analytical solution is presented below.

D.1 Description of the Simplified Model

The simplified model consists of the three algebraic and two differential equations shown below. All reaction rate constants are assumed to be constants with respect to time. The reactions are assumed to be carried out isothermally.

The overall rate of initiation, R_I, is given by:

$$R_I = 2fk_d[I] \tag{2.2.3}$$

If no inhibitors or impurities are present, equation (2.9.4) describing the concentration of free radicals, Y_o, reduces to:

$$Y_o = \left(\frac{R_I}{k_t}\right)^{\frac{1}{2}} \tag{D1}$$

If depropagation reactions are neglected, equation (2.9.3) for the rate of polymerization, R_p, reduces to:

$$R_p = Y_o[M]\, k_p \tag{D2}$$

Rate of change of the total number of moles of initiator is:

$$\frac{dN_I}{dt} = -k_d N_I \tag{2.9.5}$$

The rate of change of the number of moles of monomer is given by:

$$\frac{dN_m}{dt} = -R_p V \tag{2.9.6}$$

D.2 Derivation of the Solution to the Simplified Model

Rearranging and integrating equation (2.9.5) , as shown below,

$$\int_{N_{I0}}^{N_I} \frac{dN_I}{N_I} = -k_d \int_0^t t \cdot dt \tag{D3}$$

yields the solution:

$$N_I = N_{I0} \exp(-k_d \cdot t) \tag{D4}$$

Substituting equation (2.2.3) into equation (D1) yields:

$$Y_o = \left(\frac{2 f k_d [I]}{k_t} \right)^{\frac{1}{2}} \tag{D5}$$

Substituting equation (D5) into (D3) yields:

$$R_p = \left(\frac{2 f k_d [I]}{k_t} \right)^{\frac{1}{2}} [M] k_p \tag{D6}$$

Substituting equation (D6) into (2.9.6) yields:

$$\frac{dN_m}{dt} = -\left(\frac{2f k_d[I]}{k_t}\right)^{\frac{1}{2}} [M] k_p V \qquad \text{(D7a)}$$

Since by their definitions $[I] = N_I / V$ and $[M] = N_m / V$, equation (D7a) can be rewritten as:

$$\frac{dN_m}{dt} = -\left(\frac{2f k_d N_I}{k_t V}\right)^{\frac{1}{2}} N_m k_p \qquad \text{(D7b)}$$

Substituting equation (D4) into (D7b), rearranging, and integrating

$$\int_{N_{m0}}^{N_m} \frac{dN_m}{N_m} = -\left(\frac{2f k_d N_{I0}}{k_t V}\right)^{\frac{1}{2}} k_p \int_0^t \exp(-0.5\, k_d \cdot t)\, dt \qquad \text{(D8)}$$

yields:

$$N_m = N_{m0} \exp\left[2k_p\left(\frac{2f k_d[I]_0}{k_t}\right)^{\frac{1}{2}}\left(\frac{\exp(-0.5\, k_d \cdot t)}{k_d} - \frac{1}{k_d}\right)\right] \qquad \text{(D9)}$$

D.3 Test Case

Initial concentration of initiator $[I]_0$= 0.02 mol / L

Initiator parameters

f = 0.61

k_d = 4.5e-4 min^{-1}

Monomer parameters

k_p = 41200 L mol^{-1} min^{-1}

k_t = 2.0e9 L mol^{-1} min^{-1}

density of monomer and polymer = 1000.0 g / L

Molecular weight = 100 g / mol

If N_{m0} = 10000 mol, then at time t = 200 min. the analytical solution from equation (D9) yields:

N_m = 5504.575 or

Conversion x = (10000 – 5504.575) / 10000 = 0.44954.

The Java simulation program yields reports a conversion of x = 0.44914 when a numerical tolerance parameter of 5 is used to simulate the case presented above. The error in the program's conversion calculation is equivalent to an absolute error of less than 0.1%. As expected, the accuracy of the simulation is improved when the numerical tolerance parameter is increased. Using a numerical tolerance parameter of 8, the conversion is calculated to be x = 0.44948 which represents an absolute error of about 0.01%.

Appendix E

Source Code

The source code to the polymerization simulation program can be obtained by request to:

Dr. Marc A. Dubé, P.Eng.
Dept. of Chemical Engineering, University of Ottawa
161 Louis Pasteur St., P.O. Box 450, Stn. A
Ottawa, Ontario, CANADA K1N 6N5
Phone: (613) 562-5800 ext. 6108; FAX: (613) 562-5172
E-mail: dube@genie.uottawa.ca
Website: http://www.eng.uottawa.ca/profs/dube/dube.htm